UNIVERSIDAD CARLOS III DE MADRID

TRABAJO DE FIN DE GRADO

TITLE: Design of a mechanical assembly for power kites automatic control

Author: Alejandro Huerta Cuesta
Tutor: Gonzalo Sánchez Arriaga

June 2018

INDEX

****

FIGURES

***

TABLES

***

VARIABLES

ρ; *Air Density* $[Kg/m^3]$

C_L; *Lift Coefficient*

C_D; *Drag Coefficient*

v_a; *Apparent Velocity* $[m/s]$

v_w; *Wind Velocity* $[m/s]$

v_k; *Kite Velocity* $[m/s]$

v_t; *Tether Velocity* $[m/s]$

f; *Reeling Factor*

S; Kite Surface Area $[m^2]$

C; Basic Dynamic Load Rating $[kN]$

d_m; *Bearing Mean Diameter* $[mm]$ = *0,5* $(d + D)$

F; Real Bearing Load $[kN]$

n; Angular speed $[r.p.m.]$

P; Equivalent dynamic bearing load $[kN]$

P_u; *Fatigue Load Limit* $[kN]$

d_s; $Sheave\ Diameter$ $[mm]$

d_1; $Strand\ Diameter$ $[kN]$

F_{res}; $Sheave\ Load$ $[kN]$

r_g; $Groove\ Radius$ $[mm]$

F_{Bm}; *Medium Load* $[kN]$

F_{mr}; *Equivalen Dynamic Load* $[kN]$

$\mathrm{F_{rs}}$; *Line Pull* $[kN]$

γ; *Warp Angle*

p_{bore}; *Bore Pressure* $[MPa]$

W_{Bush}; *Bush Width* $[mm]$

D_{Bush}; *Bush Diameter* $[mm]$

F_{ss}; *Design Load (Safety Factor Applied)* $[KN]$

T_{mot}; *Motor Torque* $[Nm]$

d_{ta}; *Transmission Axis Diameter* $[mm]$

r_{ta}; *Transmission Axis Radius* $[mm]$

P_0; *Equivalent Static Load* $[KN]$

X_0; *Radial Factor*

Y_0; *Axial Factor*

C_0; *Static Load Capacity* $[KN]$

s_0; *Safety Coefficient*

μ_u; *Contamination Factor*

L_{hr}; *Rated Service Life (Rails)* $[h]$

T_a; *Alternating Torque* $[Nm]$

T_m; *Mean Torque* $[Nm]$

M_a; *Alternating Bending Moment* $[Nm]$

M_m; *Mean Bending Moment* $[Nm]$

S_y; *Yield Strengt* $[MPa]$

C_r; *Dynamic Load*

L_e; *Rated Service Life (Bearings)* $[h]$

s_r; *Stroke Length* $[mm]$

S_f; *Goodman's Stress* $[MPa]$

S_e; *Fatigue Limit* $[MPa]$

n_s; *Safety Factor*

***

ABSTRACT

Wind – generated energy is one of the most relevant "clean" energies in use today – and growing -. Use of Wind Turbines is the most extended and known way to generate energy from the wind.

An alternate and less known "wind generators" are the Airborne Wind Energy systems, which in essence consist in flying tethers or flying devices which are supposed to reach winds at altitudes impossible for standard or conventional wind turbines.

This work consists on the design of a ground station to control and measure forces in kite tethers, as a basis / first step to develop an efficient and reliable kite flight simulator and data acquisition from real flight of a kite with onboard instruments. Further, in order to make accurate simulations and properly evaluate the possible impact of an AWE system, first thing to know are the aerodynamic coefficients. This work also aims to design a modular (and transportable) ground structure to control an AWE kite, and also to take the best measures possible by means of two cell loads connected to the control lines, which with help of the data provided by onboard equipment, would be finally used to accurately determine those coefficients.

***

1. INTRODUCTION

Nowadays, as population increases, also the needs at global scale tend to increase, as may be food production, water or energy consumption. According to the World Bank Group (1), population has increased by 3 billion between 1980 and 2016. Regarding energy consumption, the International Energy Agency (IEA) estimates that the Total Primary Energy Supply was increased by a factor of 2.5 between 1971 and 2014 (81.2% by 2014); furthermore, energy was mainly obtained from non-renewable sources, such as coal or fuels of fossil origin.

Moreover, and according to data furnished by the EIA (U.S. Energy Information Administration), energy consumption will grow by a 48% between 2012 and 2040, and although the consumption of non - fossil fuels is expected to grow faster than the consumption of fossil fuels, fossil fuels still account for more than three-quarters of the total world consumption energy. Fossil fuels consumption has been rapidly increasing since the Industrial Revolution and has a main disadvantage: You can only extract energy by burning the fuel, thus releasing to the atmosphere a number of air pollutants which have direct and indirect harmful consequences on living beings and on the environment. The main sub - products released to the atmosphere are:

- CO_2
  It is the principal anthropogenic greenhouse gas that affects the Earth's radiative balance. It is the reference gas against which other greenhouse gases are measured.

- NO_x

  NO and NO_2 – both contribute to acid deposition and eutrophication which, in turn, can lead to potential changes occurring in soil and water quality. The subsequent çimpacts of acid deposition can be significant, including adverse effects on aquatic ecosystems in rivers and lakes and damage to forests, crops and other vegetation.

- SO_x

  These gases, which can easily be dissolved in aqueous media, promote the acidification of water and soil, as well as causing health problems as well as being a precursor to the formation of secondary particulate matter.

- **PARTICULATE MATTER POLLUTION**

  Composed by a mixture of organic and inorganic particles suspended in air. Depending on the measuring tools available, either PM_{10} (particles with less than 10 microns in diameter) or "fine particles", $PM_{2.5}$ (D>2.5 microns). Exposure to these

particles can improve chances of developing cardiovascular and respiratory diseases as well as –amongst other- lung cancer (2).

In Europe, the European Environment Agency has estimated that in 2013 around 467.000 premature deaths were originated by health conditions attributable to PM2.5 (3). Also, due to NO_2 and O_3 in the same year there were about 71.000 and 17.000 premature deaths respectively (3). These figures, contrary to popular belief, do not seem to show significant changes over the years. In FIG. 1, the global attributable deaths to household and outdoor air pollution for 2012 are shown. As can be appreciated this negative health effects have more severe consequences in developing countries.

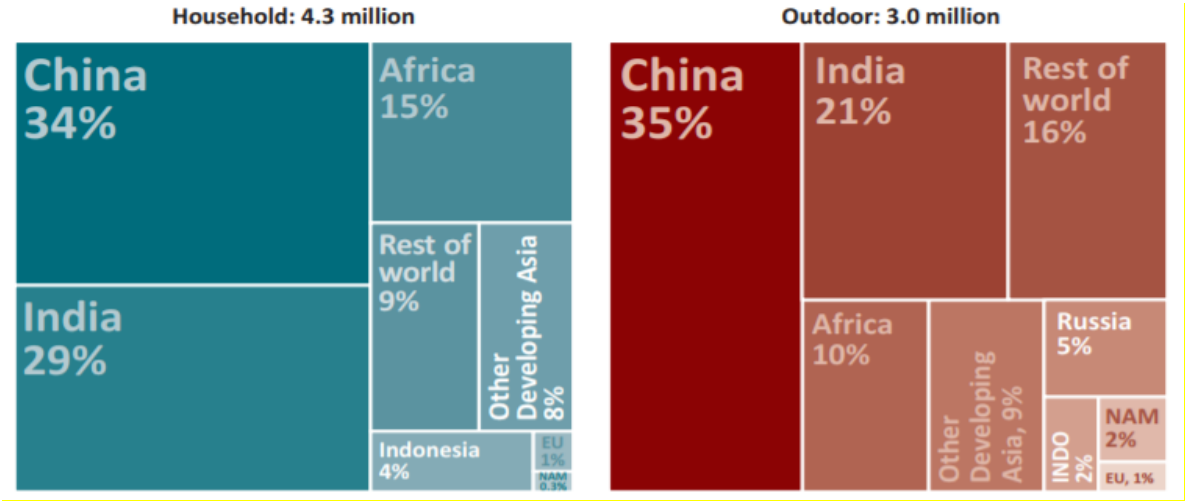

FIG. 1 REFERENCE FORM (4) GLOBAL ATTRIBUTABLE DEATHS TO HOUSEHOLD AND OUTDOOR AIR POLLUTION FOR 2012.

Notes: EU=European Union; NAM= North America; INDO=Indonesia

Another alternative, apart from fossil fuels and renewable energies, is nuclear power. It holds a small share of the global market (4.7% of world power production since 2014 (5) and global nuclear capacity is expected to grow in years to come, projected to be 402 GW to 535 GW by 2025. Whereas fossil fuels emit large quantities of pollutants, some of them previously mentioned, nuclear power has close to no greenhouse gases emission (even taking into account associated emissions from mining or refining uranium/plutonium) (6), but has a major disadvantage: It generates radioactive waste extremely harmful and difficult to manipulate.

Radioactive waste can live from a couple of hours up to several thousands of years before becoming harmless. Two types of waste can be observed, low level and high level radioactive waste. Several options are being studied and research being done; deep geological disposal seems to be the best option. Even though it may be a long-lasting solution, there is not enough data yet that can assure this kind of underground "warehouses" is safe enough and will endure long enough to prevent radioactive leaks.

The last option for energy generation goes through renewable energy sources. The IEA's electricity forecast estimates a growth of around 43% (around 920 GW) for the next couple of years (7). In years to come, solar and wind energy are expected to grow rapidly whereas hydropower may not (because major sites are already being exploited or unavailable).

Recent studies (8) show that, ideally, almost all the global power demand could be supplied if a relatively small share of the wind at geographic locations with an average wind speed of 7m/s could be exploited.

The main problem with wind power resides mainly in its high cost and the limitations of the wind turbines having a relatively low effective height where wind may not be that constant or have enough energy to harvest in an efficient way, whether horizontal or vertical configurations are chosen. Regarding wind velocity, it usually increments with height, as well as has less variability. In this context - around 30 years ago - Loyd presented and patented the idea of an airfoil or plane describing circular trajectories connected to a generator on the ground (9).

Even though this technology was "stalled" for several years, in recent times a new renewable energy technology based on this concept is emerging known as **Airborne Wind Energy (AWE)**, a community which has been growing continuously in the past decade.

1.1. State of the art

This new technology has three main approaches (10):

- *Ground-Gen Airborne Wind Energy Systems:*
  With this configuration, a two-phase cycle is used to harvest wind energy. Firstly, the airfoil ascends, generating energy, to descend later consuming a small amount of energy. This kind of operation has alternating time periods in which energy is generated and consumed, reason why the deployment of multiple AWE's in large wind energy farms is being studied.

  Two different options are being studied, a *fixed-ground-station* and a *moving-ground-station.* Even though the second option is being investigated by only a handful of Companies, some simulations show (11) that this kind of configuration can generate continuous energy on a large scale.

- *Fly-Gen Airborne Wind Energy Systems:*

  In this case energy is directly produced on-board. Even though there are not as many studies as there are with ground-gen systems, some of them show high potential, such as the M600 being developed by Makani Power, which aims to generate 600kW power (12).

The increasing importance of this new field is evidenced by the convening of International Airborne Wind Energy Conferences, the most recent having been convened in year 2017 (the 7th International Airborne Wind Energy Conference, held in Freiburg, Germany, October 2017). In this last edition researchers from 19 countries met within the framework of the EU

Marie Sklodowska-Curie Initial Training Network AWESCO (project funding 14 PhD researchers from Europe) and the Sustainability Center Freibug (13).

1.2. Socioeconomic Impact

This technology, as well as the rest of renewables, presents itself as a possible and viable alternative to fossil fuels or nuclear energy, with the potential to meet both the energy demand and lower emissions (and without having a very hazardous byproduct as nuclear power). However, and since this technology is still under development, is difficult to assess the economic implications and potential barriers (14).

According to recent studies (15), renewable energies have different impacts that have to be regarded before a project carried out. Effects on landscape, wildlife or air pollution are the main indicators to take into account. Of these, landscape and wildlife impact are the most highly regarded effects of renewable technology, wildlife usually over landscape (16). In this case, AWE systems should offer a better solution since the impact on the landscape should be less than the effect of conventional wind turbines and their operational heights may prevent birds from colliding with the systems during operation (as it happens with conventional wind turbines).

1.3. Objective

To make accurate simulations and evaluate the possible impact of an AWE system, first the aerodynamic coefficients must be known. This works aims to design a modular ground structure to control a kite and to take the best measures possible by means of two cell loads connected to the control lines, which with the help of the data provided by onboard equipment, would be finally used to determine those coefficients.

The present project has been developed and designed looking for the possibility to adapt the structure to changes and serve as a basis for further improvements without having to redesign the whole system (hence the "modular" approach). With this premise in mind the design has been separated in three modules as following:

MODULE I: Or *front* module, this module along with MODULE-III will withstand most of the forces exerted by the kite. It contains the sheaves that will act as a derivative mechanism helping to direct and maintain the tether in a horizontal plane to minimize potential errors in the load cells.

MODULE II: Supports the rails and has been devised in a way that the load cell end is aligned with the sheaves. It`s the module that will support the cell loads.

MODULE III: This module acts as a support/housing of the electromechanical drive. For the current project no reducer is used, but with higher loads it may be needed. In this situation it would be easy to redesign module III without having to recalculate the other two modules (taking into account the limitations of the other two modules). In FIG. 2 the modules and its components can be found:

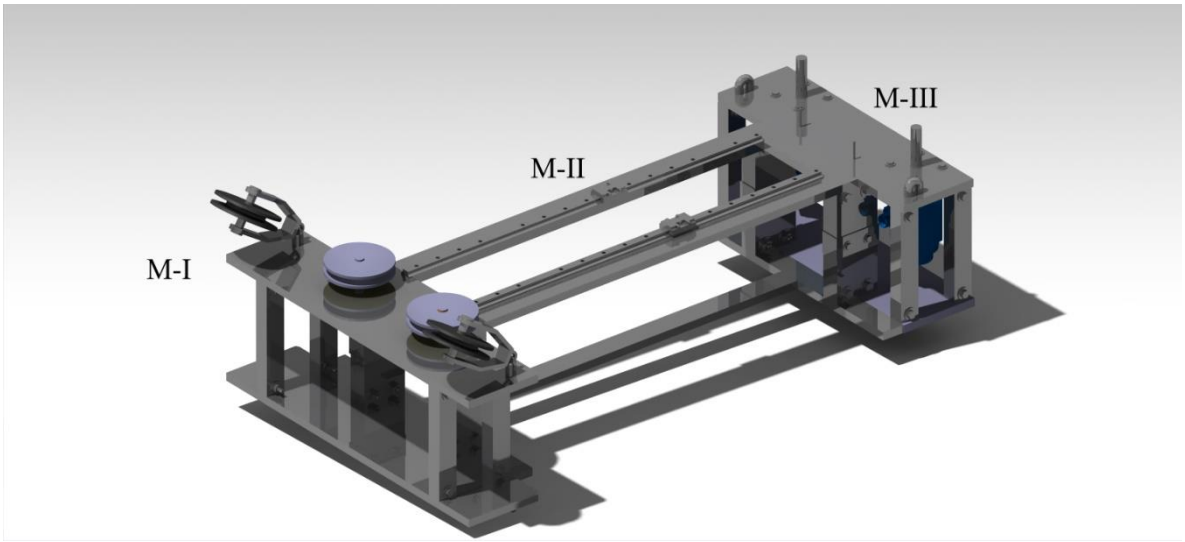

FIG. 2 MODULES AND THEIR COMPONENTS

Every module has the possibility of adding counterweights to prevent the structure from moving. In Module-III part of the space would be used by the batteries needed to power the electric actuators, acting as well as counterweights on their own.

***

2. BACKGROUND & THEORETICAL MODELS

2.1.System Requirements

In order to set a procedure to dimension a kite test bank, several conditions must be met for the whole system to work properly, minimize errors and assure the desired service life. In this chapter 2, a general view of the main design parameters accounted for when dimensioning the components is reviewed, as well as an introduction to the main design concepts and considerations of each individual component, that will be later developed (see 3 Preliminary Design).

Main Considerations

- *Location:* Flying a kite of determined wingspan cannot be done safely indoors, so the first condition that should be met is the capacity of the structure and components to endure outdoor working conditions providing good service life with the lowest possible maintenance. For this every individual component has to be studied and supposed to work in the least favorable conditions, making use of seal or providing protective coating (among other possible measures) if required.
- *Maximum Height:* The maximum height taken into account by the present work corresponds to the tether length. The tether is supposed to withstand the loads at which it will be subjected and since the wind velocity has been calculated for an altitude of 25 m (see 2.2 **Wind Models**), that would be the maximum tether length and thus the maximum height.
- *Movement Limitations:* Maximum and minimum azimuth and elevation angles constraint the physically possible and admissible flight path of the kite. Later on this limitations will be studied and a fixed value obtained (see 2).
- *Temperature Operation:* The design temperature range has been set between 15ºC and 40ºC. Outside this range the structural stability and performance of the components cannot be assured by the present work.
- *Design Load:* In order to perform the calculations for each element, loads at which the components will be subjected have to be studied. This operational load is calculated later in this work (see 2.3 **Assumptions & Considerations**)
- *Dimensions:* The maximum dimensions will be defined by the means of transportation in which the test bench is intended to be carried. The reference vehicle for the dimensioning has been a medium – size car, a 4 x 4 Skoda Octavia Scout, with the following characteristics:
  Total Load Volume (folded back seats): 1825 liters
  Trunk Dimensions: 1170 x 1660 x 940 mm
- *Service Life:* Maximum service life is desired for each component. So as to assure this condition, the components have been preliminarily designed for *infinite life*, later making modifications (if necessary) for them to comply with the rest of the structure.
- *Maximum Admissible Load (Vehicle):* Depending on the material chosen, weight of the structure may be too heavy for a standard car (in this case a four wheel drive Octavia) to transport, generating potential risks for the driver. Final weight of the product has been checked and does not exceed the load capacities of the indicated vehicle.

- *Anchorage:* If the weight of the structure is not enough, the forces exerted by the kite may cause it to displace, generating risks for the people doing the tests. For the structure and since the operational range of the structure must be as wide as possible, space in each module is available for counterweights to be used.

2.2. Wind Models

In general, wind velocity decreases as it approaches ground level. Despite wind's variable nature, its velocity usually increases with altitude, which is referred to as *wind shear* (17). Based on this micro - phenomena occurring over relatively short distances, several models have been proposed:

- ***LOGARITHMIC LAW (LL)***

$$\omega_{(z)} = \frac{\mu}{k}\left[\ln\left(\frac{z}{z_0}\right) - \Psi_m\left(\frac{z}{L}\right)\right] \qquad (1)$$

- ***POWER LAW (PL)***

$$\omega_{(z_2)} = \omega_{(z_1)}\left(\frac{z_2}{z_1}\right)^{\alpha} \qquad (2)$$

Generally, the PL model shows better accuracy at lower heights then the DH model, although the DH model has been proven to be far more efficient at extrapolating wind speed for higher heights (the DH model exhibits biases reducing from 6% (40 m) to 2% (80 m) and 1% (140 m) and biases decrease from 20.32% (40 m), to 6.06 (80 m) and 6.16% (140 m) when predicting extrapolated **AEY** (18)**.** Since generally for the tests going to be performed to obtain precise tether force measurements, the kite won´t go further than 40/50m, the PL (2)was used when extrapolating wind speed.

Example: with data taken from a weather station located in Rascafría, Madrid (19), from the data obtained from the weather station and applying the PL (2) the wind speed at the height desired can be computed.

TABLE 1 WEATHER STATION

Location	Rascafría, Madrid
Device I.D.	3104Y
Height [m]	1159
Latitude	405323 N
Longitude	035318 W

The wind speed at the desired height can then be calculated by means of Table 1 and (2 :

$$v_w = 11\ m/s$$

2.3.Assumptions & Considerations

Before dimensioning the components that will compose each module, the maximum load to which they are going to be subjected has to be calculated, this in order to prevent static or dynamic failure. In order to estimate the maximum load some simplifications are assumed (see Table 2), such as constant wind velocity, parallel to the ground and cte C_D and C_L, assumed constant for a fixed attack angle of 25º (in reality these coefficients may vary with the instantaneous attack angle). In Table 2 the considerations and assumptions taken for computing the forces and velocity are accounted for.

TABLE 2 ASSUMPTIONS & CONSIDERATIONS

Assumptions & Considerations	
1	Wind has constant velocity and direction with uniform profile
2	Well established airflow over the kite
3	Air density is 1.225 $^{Kg}/_{m^3}$
4	Tether is straight and massless
5	Tether drag is neglected
6	Tether only transmits traction forces
7	Finite wing with fixed geometry
8	Massless kite
9	Moment coefficients are neglected (does not contain a bridle)
10	C_L Constant for 25º
11	11 m/s Wind Velocity
12	Approximate area of the kite 20 $[m^2]$

2.4.Tether Force

The force transmitted by the tether has to be known before starting to dimension any of the components of the system. For the test bench it will be calculated from the study published by Schmehl, R. et al (20), stating that the force in a tether can be computed as:

$$F_t = \frac{1}{2}\rho C_R v_a^2 S \qquad (3)$$

With C_R as:

$$C_R = \sqrt{{C_D}^2 + {C_L}^2} \qquad (4)$$

Being C_L and C_D lift and drag coefficients respectively.

With the data provided in Table 2 tether force stays as:

$$F_t = 0.945\ KN$$

2.5.Tether Velocity Calculation

Also from the same study (20), the tether force can be calculated. It presents a general relationship between apparent air velocity and real air velocity, as follows**:**

$$v_a/v_w = (sin\theta cos\emptyset - f)\sqrt{1 + (F/D)^2} \qquad (5)$$

Knowing the reeling factor:

$$f = v_t/v_w \qquad (6)$$

Tether velocity, v_t, can be computed as:

$$v_t = v_w sin\theta cos\emptyset - \frac{v_w}{\sqrt{1 + (F/D)^2}} \qquad (7)$$

In the reference to the rest of the parameters can be found (***F*** and ***D*** are lift and drag forces respectively). Maximum tether velocity will be then set as:

$v_t = 7\ m/s$ (for $\theta = 30º$ and $\emptyset = 0º$)

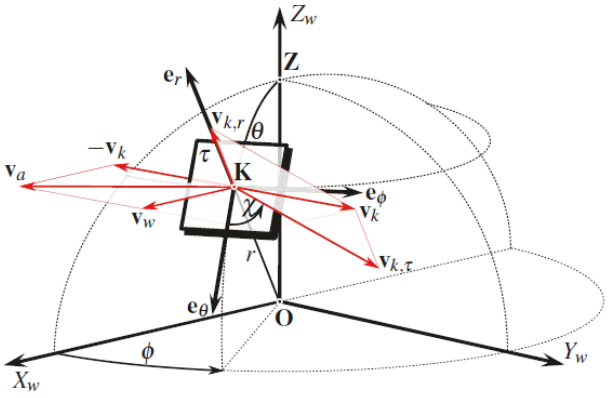

FIG. 3 – VELOCITIES DECOMPOSITION. REFERENCE FROM (20)

3. PRELIMINARY DESIGN

For dimensioning the structure first, the operational requirements (see Preliminary Design) must be carefully understood to choose configurations, solutions and materials. Before designing the modules, loads and dimensions of the main components to be mounted must be known since it will condition entirely the geometry, size of the components and specifications of the modules. In this chapter the sheaves, bushings, bearings, rails and AC actuator are subject to a preliminary study from where the final design of each of the modules will be done. Even though in chapter 3.6 **Materials** several tables corresponding to each module can be found, in the description of the main elements is included its location in the test bench.

3.1. Preliminary Design Conditions

The following table is a summary of the design considerations for the test bench main components:

TABLE 3 DESIGN CONDITIONS

Working atmosphere	Dirty
Maximum Dimensions	116x117x94 $[cm]$
Maximum Operating Wind Velocity	14 $[\mathrm{m}/s]$
Maximum Area of the kite	20 $[m^2]$
Working Temperature	15-40 $[ºC]$
Maximum Height	25 $[m]$
Safety Coefficient, n_s	1.7
Load_{ss}	1.01 $[KN]$
Tether Velocity	7 $[m/s]$
Gravity	10 $[m/s^2]$

With these conditions the main components can be designed, obtaining the main values necessary for the design of the modules.

3.2. Sheaves

4 sheaves have been designed for the System, two intended to change the forces from the vertical to the horizontal plane (FIG. 4 Sheaves Top View, components A), and two other intended to change the force direction towards the rails where the cell loads would be installed (FIG. 4 Sheaves Top View, components B). This section introduces the main design parameters, characteristics and considerations taken into account as per the relative regulation (DIN 15061).

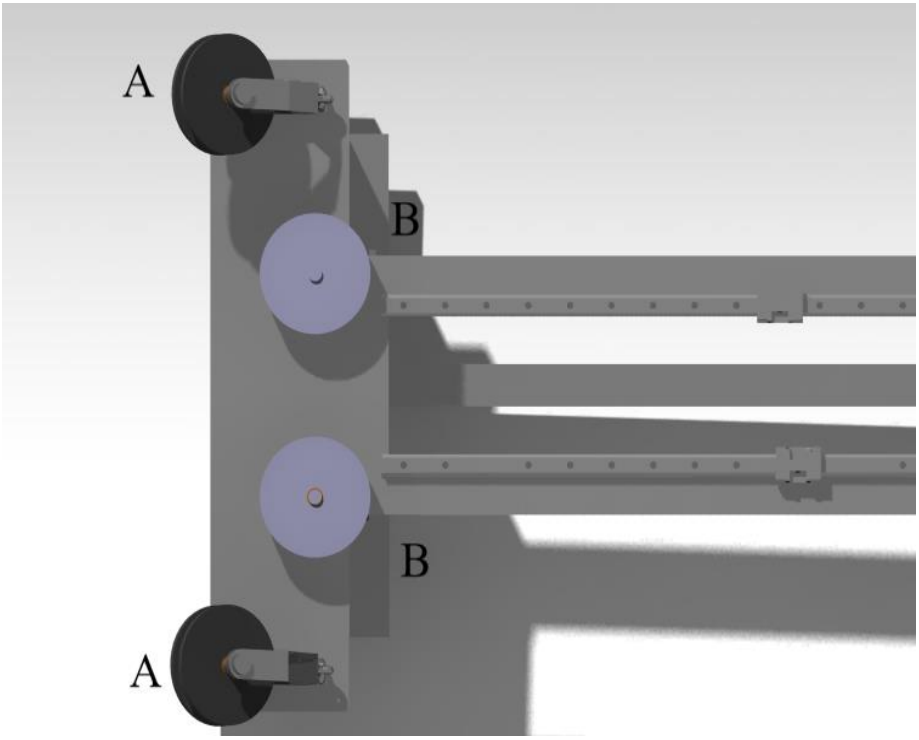

FIG. 4 SHEAVES TOP VIEW- COMPONENTS "A" AND "B"

Sheaves usually have a groove in the inner surface, assuring the tether always stays in the desired position. They are usually used for lifting loads, transmitting power or, as in this case, redirecting the direction of a load. They must be carefully designed to optimize service life of both the test bench and the pulley. An over dimension would cause an overpriced solution and if not designed with care, unexpected failure may cause problems during operation and safety risks, problems and risks that can be easily avoided.

The lifetime of sheaves is heavily influenced by Hertzian Pressure, line pull, sheave diameter, groove profile and sheave material (21). Commonly sheaves can be found in steel, aluminum or nylon, the later ones a relatively new trend. Cast nylon sheaves provide improved life service as well as high compressive and tensile stress. They are also corrosion resistant, avoiding rust and preventing the need of a protective coating. Furthermore, they present the best weight/strength ratio compared with aluminum or steel cast sheaves.

In this particular case the pressure generated in the groove of the sheave is sufficient to use a nylon sheave. As general design rules for sheaves, the following have been followed (21):

- Groove diameter should exceed the wire rope diameter by at least 5%, assuring good support of the tether.
- The depth of the groove should be over 1.5 times rope diameter to prevent jumping.
- The groove angle of 45º assures best support to the cable.

For the selection of the optimal sheave, the bore pressure (that will be used in later calculations when designing the bushings) and groove pressure (to select the best material)

must be calculated. According to the current regulation and the manual provided by TIMco (21), the main parameters have been computed as follows:

3.2.1. Sh*eave Load*

$$\mathrm{F_{rs}} = 2F_{ss} sin\left\{\frac{\gamma}{2}\right\} \qquad (8)$$

Where $\mathrm{F_{rs}}$ is the "line pull" or force generated on the sheave's axis as a function of the warp angle, and γ is the warp angle.

TABLE 4 LINE PULL

γ [º]	30	90	120
F_{rs} [KN]	0.182	1.68	0.617

As can be observed from the values in Table 4 the maximum value is obtained for a warp angle of 90º.

3.2.2. Groove Pressure

Groove pressure is necessary to determine sheave's material, however and since the tether diameter[1] is around 0.055 times sheave tread diameter, it can be ignored (21)

3.2.3. Bore Pressure

$$p_{bore} = \frac{\mathrm{F_{res}}}{D_{Bush} W_{Bush}} \qquad (9)$$

Where d_1 stands for the bushing outer diameter and W_{Bush} for the width. A bushing is preselected and later in this chapter the operational conditions are evaluated to check if the can be met. Following these premises, sintered bronze bushing provided by SKF PSM 182430 A51 has been preselected. In Table 5 (see **Bushings**) the main constructive dimensions for the bushing can be found. Bore pressure will then be:

$$p_{bore} = 2.333\ [N/mm^2]$$

[1] S-Core tether (43)

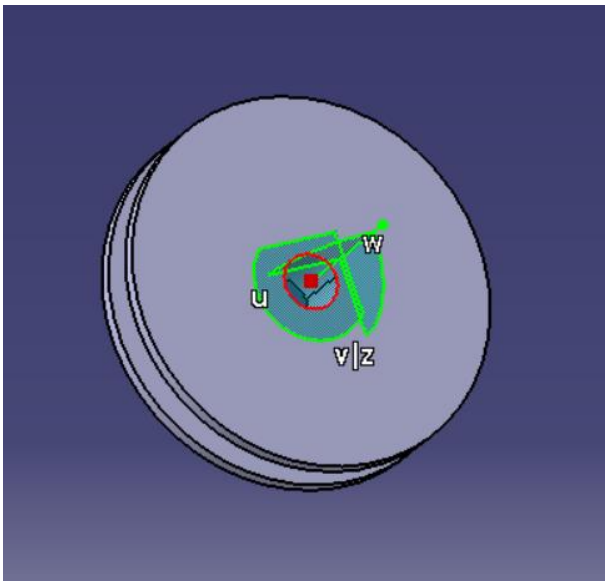

FIG. 5 REPRESENTATION OF THE SHEAVE

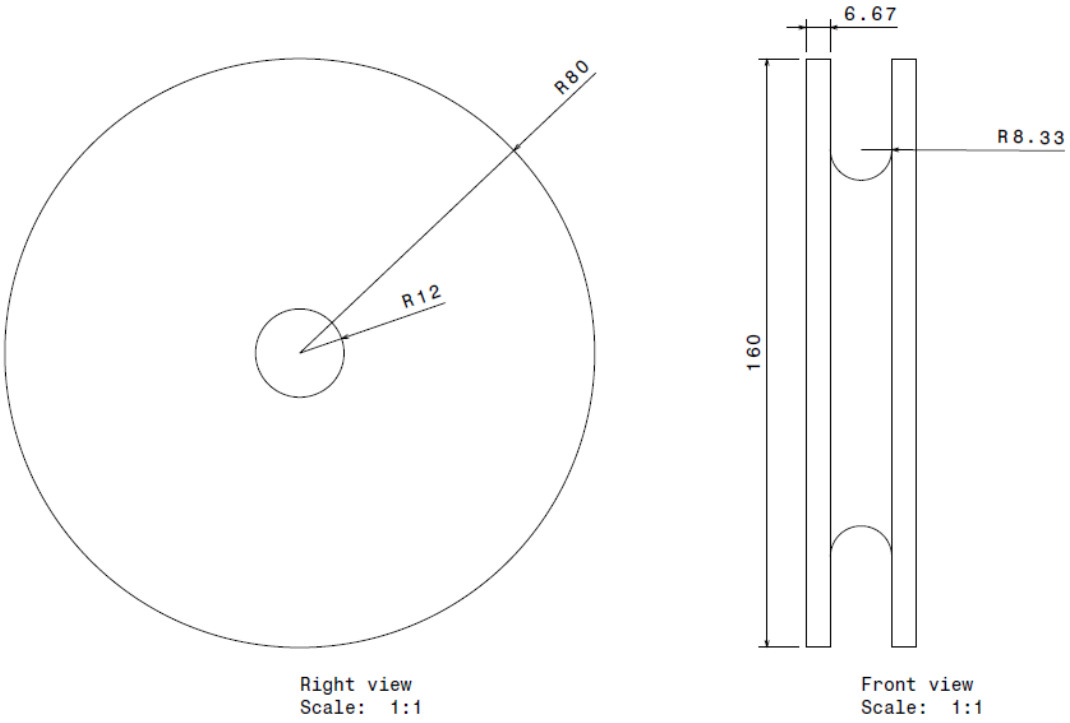

FIG. 6 CLIP OF THE SHEAVE DRAWING (GENERATED WITH CATIAV5)

3.3.Bushings

Bushings or plain bearings are components that, with a reduced cost when compared to other solutions as might be bearings, prevent contact between two surfaces of different machine components. The bushing selected for the current application, a sintered bronze bushing produced by **SKF**, fulfills the load requirements since it has a wide temperature range and the maximum permissible load is way higher than that the bushing will be subjected to (25 N/mm^2) (22). In this kind of bearing, lubrication plays a major roll, and friction coefficient is highly influenced by the chosen type of lubrication. Typically, bronze bushings are grease lubricated, helping prevent wear and corrosion and since the test bench may operate in heavily contaminated atmospheres, installation of seals is highly recommended to prevent malfunctioning and failure of the bushings.

TABLE 5 BUSHING CHARACTERISTICS

Product	$d_{Bush}\ [mm]$	$D_{Bush}[mm]$	$W_{Bush}[mm]$
PSM 18243 A51	18	24	30

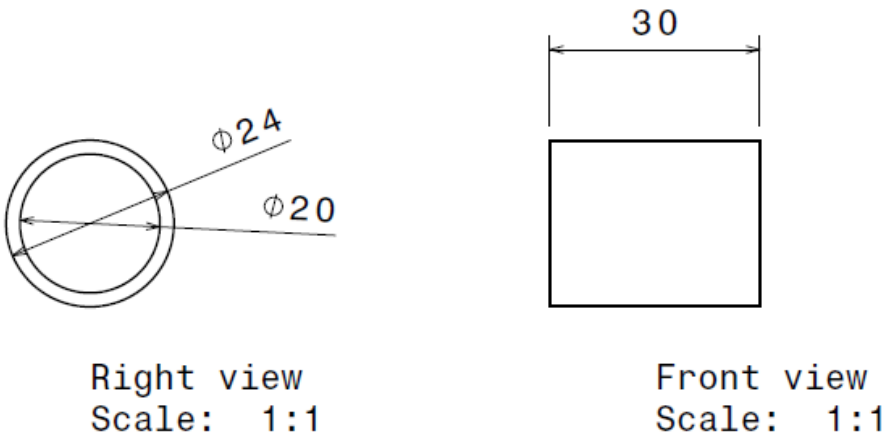

FIG. 7 - CLIP OF BUSHING DRAWING (GENERATED WITH CATIAV5)

3.4.Actuator

Controlling the kite is a challenging question since several requirements must be met. The control system does not only have to support the stresses and loads generated by the line pull but also must have good response time to change directions. Pneumatic drives, for example, offer a good solution to applications with simple controlling movements, with a proven technology and safety since virtually no hazardous situation may arise from a failure.

Hydraulic drives, on the other hand, offer a solution to application where high loads are needed, and the same system can be used for several purposes. Even so, hydraulic devices

still don´t have the kind of response searched for the control of a kite and the failure may derive in dangerous situations (picture an oil leak from the system: fire and slip hazards arise).

The best solution would be an electromechanical drive, since it can be found for a wide range of loads and velocities and improved control can be obtained by the implementation of frequency converters that change the polarity of the motor thus making it able to turn in both directions, optimizing control of the system.

3.4.1. Considerations and selection

An electric actuator is a device that converts electric energy into mechanical torque. By use of converters (which are not studied in this work), the power output can be controlled and the polarity of the motor reversed, obtaining an actuator with the capacity to adapt to almost any system requirements.

Several factors must be taken into account:

- Mechanical Power: Output the drive must have to control the system
- Velocity: Speed (in r.p.m.) at which the motor can operate
- Torque: Force at which a motor turn. For this application a motor with a brake would be a better choice to control the position of the kite.

3.4.2. Servomotor

Servomotors are the best solution possible for the test bench. They present compact design, low inertias and the possibility to control both position and velocity, thus making them the optimal choice for the system since it is relatively easy to implement a control system and since they work with DC, they can be powered by batteries which is perfect for a system intended to work outdoors.

For choosing the best product, first the minimum conditions to be met must be known. Firstly, the minimum power needed by the motor to withstand and operate the kite must be higher than the power the kite is generating. Equation (10) shows the minimum power required[2]:

$$P_m = F_{ss} v_t \qquad (10)$$

Which in this case would result in:

$$P_m = 7.1\ kW$$

[2] If the conditions differ from the ones stated in Table 3 the servo must be revised.

Once the power required is known, the torque the motor has to endure has to be calculated. Setting an initial diameter for the transmission axis, which later will be subjected to a fatigue study to determine its service life, of 40 mm, the torque at which the motor will be subjected is determined by:

$$T_{mot} = d_{ta} F_{ss} \tag{11}$$

So, the torque the motor must withstand is:

$$T_{mot} = 40.4\ Nm$$

The operational velocity of the kite should be around a third of the wind velocity. Taking as reference the wind velocity from Table 3 the operational speed at which the servo will be working would be:

$$n = \frac{60\left(\frac{1}{3}\right) v_w}{2\pi r_{ta}} \tag{12}$$

After substituting each term, the velocity at which the motor should operate would remain as:

$$n = 1114.08\ \text{r. p. m.}$$

After computing the operational requirements, the final motor can be chosen. Table 6 summarizes the design conditions and the product selection (as well as the supplier, in this case Omron).

FIG. 8 -MOTOR - CAD MODEL PROVIDED BY OMRON FROM REFERENCE (23).

TABLE 6 SERVOMOTOR

Design Requirements	
Operational Torque	40.4 Nm
Power	7.1 kW
Operational Velocity	1114.08 r. p. m.
Product overview	
Provider	Omron
Model	R88M-K7K515C-BS2
Rated Torque	47.8 Nm
Capacity	7.5 kW
Nominal Velocity	1500 r. p. m.

3.5.Bearings and rails

In this section the main parameters for selecting the correct bearing and rail are explored, as well as the final choice for the system and the recommended product and its provider.

3.5.1. Bearings

Bearings are components designed (as bushings) to prevent contact between moving parts in a machine. Usually bearings withstand the reactions of an axis and must be of the lower size possible, so their construction and mechanical properties have to be excellent. When selecting a bearing, several factors have to be accounted for such as type of load, direction of the load, mounting space or operational velocity among others. For this project, they will be mounted on Module-III (see FIG. 9)

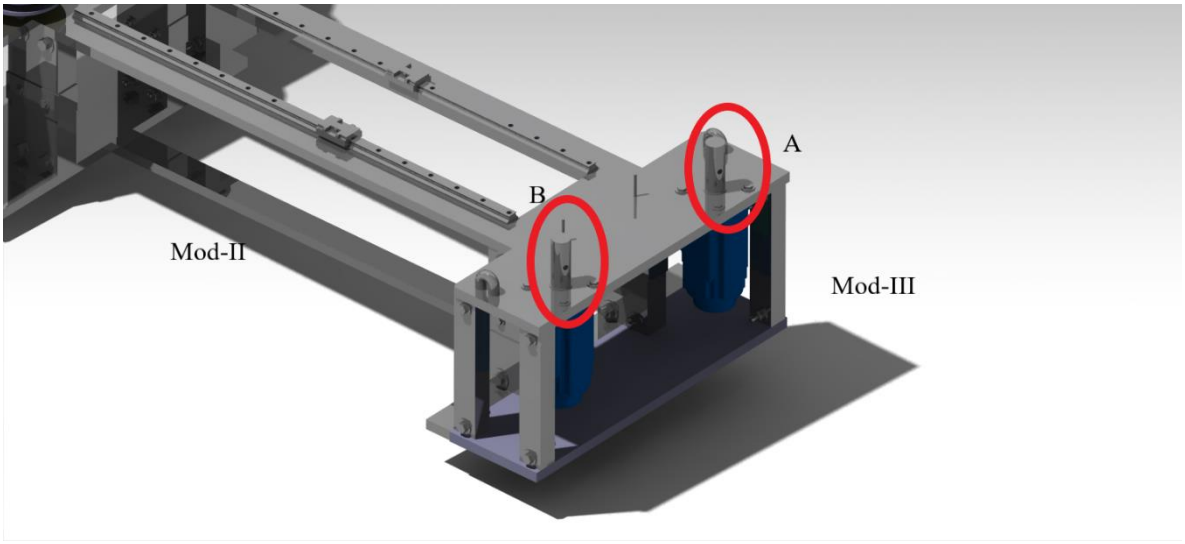

FIG. 9 - BEARINGS POSITION ON MODULE III (A AND B)

To select the correct bearing or set of bearings several calculations must be done to check both static and dynamic conditions. Provided the static conditions are met, a dynamic check

will be done and once the dynamic behavior of the bearing is deemed acceptable the service life (in which lubrication plays a major role) will be checked.

Static Check

To perform the static check first the equivalent static load, P_0, must be computed. Since the bearings are going to be subjected to alternating forces, to compute the equivalent static load first the medium load, F_{Bm}, has first to be computed:

$$F_{Bm} = \frac{F_{min} + F_{max}}{3} \qquad (13)$$

With F_{min} and F_{max} being respectively the maximum and minimum values in Table 4, which means F_{Bm} has a value of 1.86 KN.

F_a, On the other hand, is the force in the direction of the rotation axis. The weight of each component can be easily obtained if the material is defined (for the purposes of this work we have done so by using the already cited tool CatiaV5). As will be justified later in this work, most of the components would be made of steel. FIG. 10 shows a clip from the CatiaV5 model in which the weight can be clearly distinguished.

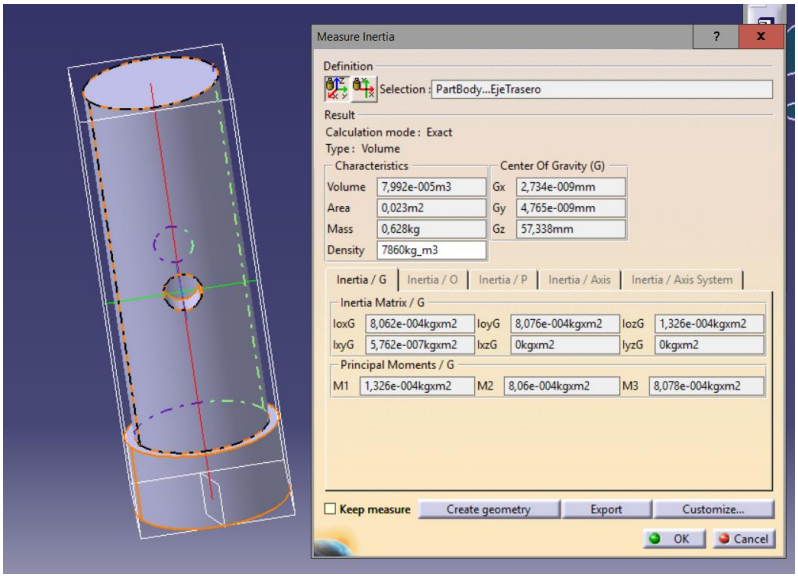

FIG. 10 TRANSMISSION AXIS – DESIGN DRAWING WITH MASSES AND MEASURES

Once the weight is known, F_a can be computed with a value of 6.28 N. X_0 and Y_0 are the radial and axial factors respectively. For single bearings, X_0 has a value of 0.5 and Y_0 for single bearings and a contact angle of 15º would be 0.46 (24).

nd substituting in (14) P_0 value will be

$$P_0 = X_0 F_r + Y_0 F_a = 0.5 F_{Bm} + 0.46 F_a \quad (14)$$

$$P_0 = 0.934 \text{ KN}$$

In Table 7 the recommended safety coefficients, S_0, for each type of bearing and operation presented.

TABLE 7 STATIC SAFETY COEFICIENTS. REFERENCE FROM (24)

	Moving Bearings				Fixed Bearings			
Working requirements	No importance		Normal		Superior			
	Balls	Cylinders	Balls	Cylinders	Balls	Cylinders	Balls	Cylinders
Smooth	0.5	1	1	1.5	2	3	0.4	0.8
Normal	0.5	1	1	1.5	2	3	0.5	1
High transient Loads	≥1.5	≥2.5	≥1.5	≥3	≥2	≥4	≥1	≥2

And knowing the safety coefficient is determined by the following formula:

$$S_0 = \frac{C_0}{P_0} \quad (15)$$

The static load capacity, C_0, can be computed. Note that the static load capacity of the selected bearing must be at least equal to the one resulting from:

$$C_0 = S_0 P_0 \quad (16)$$

So, for a superior working bearing with moving bearings, the minimum static load capacity must be of $C_0 = 1.87\,kN$. In the following table the best options for the design, provided by SKF, are shown:

TABLE 8 BEARINGS. PROVIDER SKF GROUP. FROM REFERENCE (24)

Principal Dimensions			Load Capacity		Limit Fatigue Load	Mass	Product
d_b $[mm]$	D $[mm]$	B $[mm]$	C $[kN]$	C_0 $[kN]$	P_u $[kN]$		
40	52	7	4.49	3.75	0.16	0.032	61808
	62	12	13.8	10	0.425	0.12	61908
	68	9	13.8	10.2	0.44	0.19	16008

Since it is the smaller, bearing 61808 will be preselected.

Dynamic Check

Provided that the static conditions are met, a dynamic check is made to estimate the service life of the bearing working under the system conditions. For doing so first the equivalent dynamic load, P, must be computed following one of the following criteria:

$$P = F_{Bm} + 0.55F_a; \quad \frac{F_a}{F_{Bm}} \leq 1.14 \qquad (17)$$

$$P = 0.57F_{Bm} + 0.93F_a; \quad \frac{F_a}{F_{Bm}} > 1.14 \qquad (18)$$

Since the factor $\frac{F_a}{F_{Bm}}$ is lower than 1.14, equation (17) is used. The dynamic equivalent load then would be:

$$P = 1.87\ KN$$

According to ISO 281:2007, the extended life service (in hours) of a bearing can be calculated as follows (24):

$$L_e = a_1 a_{SKF} \left(\frac{C}{P}\right)^{3^3} \frac{10^6}{60\ n}\ \ h \qquad (19)$$

Where a_1 represents the reliability, that for a 97% would be around 0.47(pag 65 in SKF Bearing Manual (24).

The coefficient a_{SKF} depends on the viscosity relation, k, which relates the nominal viscosity of the lubricant and real operating viscosity and the contamination factor. Even though the bearing should be mounted with seals, what should prevent any foreign particle from entering the lubricant, a slight contamination factor, μ_u, is going to be taken into account (set around 0.6 for the condition mentioned).

Using the diagrams that can be seen in SKF bearings catalogue[4] (pages 72 and 73 from (24)), the real operating viscosity would be $\vartheta = 18\ {mm^2}/{s}$ (with $0.5(d_b + D)$ according to bearing 61808 and the operating velocity from Table 6). Assuming a working temperature of 65º, the lubricating oil must be at least of a viscosity according to ISO VG 46.

After all the data are known, the coefficient a_{SKF} (that can be found from a diagram on page 69 in SKF bearing manual (24)) for this case is:

[3] For ball bearings. For roller bearings would be 10/3

[4] The contents of the document (24) are specifically forbidden from being reproduced without SKF's authorization.

$$a_{SKF} = 2.1 \text{ (with } k = 2.5 \text{ and } \mu_u \frac{P_u}{P} = 0.051)$$

And thus, the estimated service life for the bearing would be:

$$L_e = 200 \text{ h}$$

3.5.2. Rails

Rails, as bearings and bushings, minimize the friction forces between two relative moving elements of a machine but, in contrast with the other two, rails are designed for linear movements. In the test bench they are located on Module-II (see FIG. 11). FIG. 12 shows the runner block which run on each rail.

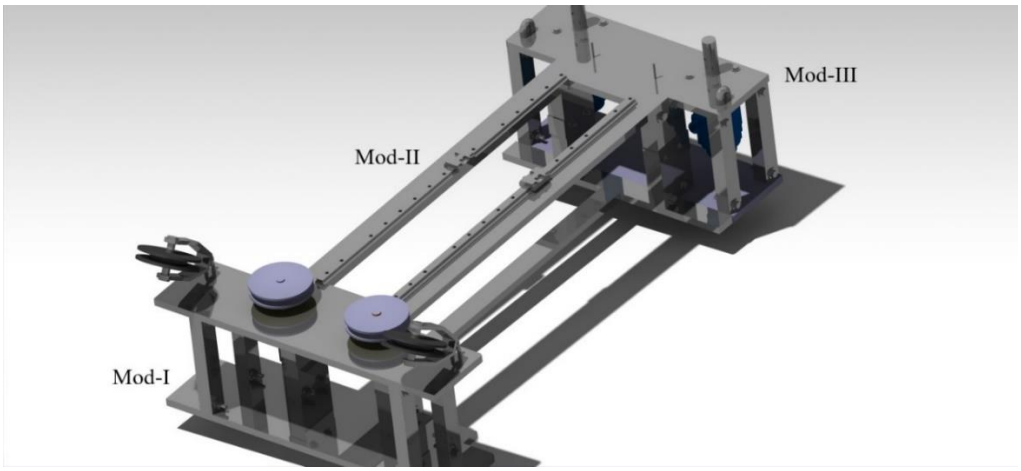

FIG. 11 LOCATION OF RAILS IN MODULE-II

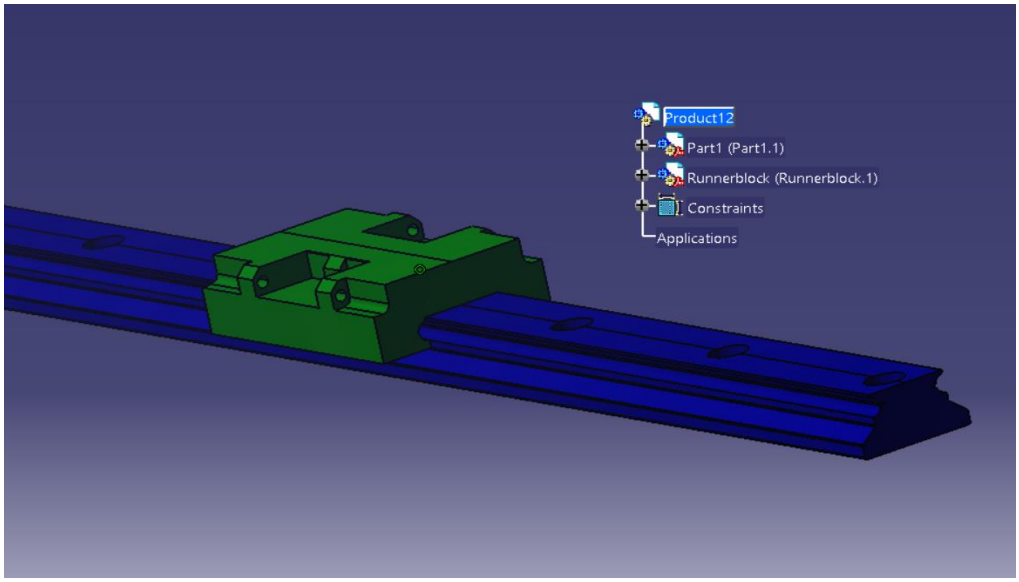

FIG. 12 RAIL/RUNNER BLOCK ASSEMBLY (POSITION OF RUNNER BLOCK ON EACH RAIL, RUNNER BLOCKS MOVE BACK AND FORTH)

FIG. 13 shows the main differences between the available rails. It can be clearly seen that the best options for the assembly would be either a fluid static sliding guide, or a magnetic guide. However, fluid static guides do need a pumping station so the fluid between surfaces has enough pressure to withstand the weight thus preventing contact between surfaces. This makes these systems expensive (furthermore, the pumping station and circuit are sensible equipment prone to failure if not correctly maintained and in fail case, inadequate lubrication regime will appear, increasing friction forces thus making the load cell measurements inaccurate.

Magnetic suspension, apart from being the most expensive option, is not fully standardized so there is not a norm yet to design the rail. Taking into account these facts, the best option to comply with the regulation and the operational requirements, the best sliding guide would be roller or ball guides and runner blocks provided with seals and internal lubrication.

For the installation of the rails some conditions must be regarded to avoid a premature failure of the rail or of the adjoining structure, or of both. When bolting together the rail and supporting structure, residual stresses appear, which alone or in combination with external forces may cause plastic deformations in the structure or in the contact surfaces. One way to prevent plastic deformation of this kind would be to assure a high area contact between rail and structure, meaning a high surface finish in both products is demanded.

TABLE 9 RAILS CHARACTERISTICS

Characteristics	Rolling contact guides			Hydrodynamic sliding guides		Fluidostatic sliding guides		Magnetic guide
	Ball guide	Roller guide	Cam roller guide	Metal/ metal	Metal/ plastic	Hydrostatic guide	Aerostatic guide	Magnetic suspension
			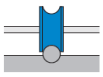	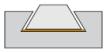	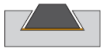			
Load-bearing capability	+++	+++	++	+++	+++	+++	o	+++
Rigidity	++	+++	+	+++	++	+++	o	+
Accuracy	++	++	++	+	+	++	++	+++
Friction characteristics	++	++	++	+	+	+++	+++	+++
Speed	+++	+++	+++	+	+	+++	+++	+++
Damping characteristics	+	+	+	+++	+++	+++	+++	+++
Operating safety	+++	+++	+++	+++	+++	+	+	+
Standardization	+++	+++	+++	+	+	o	o	o
Service life	++	++	++	++	++	+++	+++	+++
Costs	++	++	++	+++	+++	+	+	o

+++ Very good
++ Good
+ Satisfactory
o Adequate

FIG. 13 RAILS CAPACITY. COMPARISON TABLE. FROM (25)

Since the rail will only be subjected to the weight of the load cell, a miniature rail system can be used. Usually these systems have a maximum distance of 1000 mm, which is enough for the control of the kite since only around 500 mm are needed to fully control the kite. Miniature systems have the disadvantage of operating between 3 m/s and 5 m/s (26), but

for controlling a kite with winds of 14 m/s is enough since as stated earlier in this document, the control speed of a kite is close to a third of the wind speed, condition that is fulfilled in this case.

Similar to the case of the bearings, the service life (in hours) of the rails can be calculated from (26):

$$L_{hr} = \frac{10^5 \left(\frac{C_r}{Fmr}\right)^3}{2\ s_r\ n_s\ 60} \qquad (20)$$

Where C_r is the dynamic load capacity, Fmr the equivalent dynamic load capacity, s_r the length of the stroke and n_s the stroke repetition rate.
The following table offers a summary of the size, weight and load capacities of the runner block:

TABLE 10 RUNNER BLOCK

Size	20
Load Capacity	7.9 KN
Mass	0.177 Kg

Knowing the length of the stroke must be 500 mm and assuming a stroke repetition rate of 5 min^{-1}, equation (20) would result in:

$$L_{hr} = 2.05E10\ h^5$$

This value would be too high in other circumstances, but the comparison of the efforts the runner block is designed to withstand and the ones it will be operating with in the test bench make the service life of the component unusually high.

The same lubricant as with the bearings can be used for the rails. The runner block has 4 lube tubes from which the lubricant must be replenished when needed.

3.6.Materials

The selection of the correct material for the components plays a major role in this project. All three modules must be able to work in an outdoor environment, meaning they should be able to endure wear and corrosion from being exposed to humid atmospheres or impacts of small particles (for example sand particles carried by the wind). Bearing this in mind, this

[5] Mass of the cell load has been taken as 2kg

section offers a comparative between steel and aluminum for the main modules, protection against wear or/and corrosion (if needed).

Not only resistance to external conditions is evaluated in this section, but also mechanical strength and weight, since the modules are intended to serve as basis for a system that might be further developed so not only they would have to withstand the stresses generated by the kite but they should also have a good margin so modifications in the components can be made without modifying the main structure.

3.6.1. Steel vs Aluminium

Different behaviors can be observed in most metals when subjected to external stresses. As a reference, they can be separated in brittle and ductile materials. Brittle, for example, materials do not show plastic deformation when subjected to high stresses and fail upon reaching the Ultimate Tensile Strength (FIG. 14) (S_u).

Ductile materials, as opposed to brittle materials, do deform plastically before reaching S_u. They also have a measurable, well-defined Yield Strength (S_y), which is the maximum stress that can be applied before plastic deformation occurs (FIG. 14). Before reaching S_y, it behaves elastically, meaning that after removing the load/stress which the solid is being subjected to goes back to its original shape, length or volume. When entering the plastic region, instead of recovering, non-reversible deformation starts taking place. Plastic deformation is characterized by a strain hardening region and a necking region, finally reaching fracture.

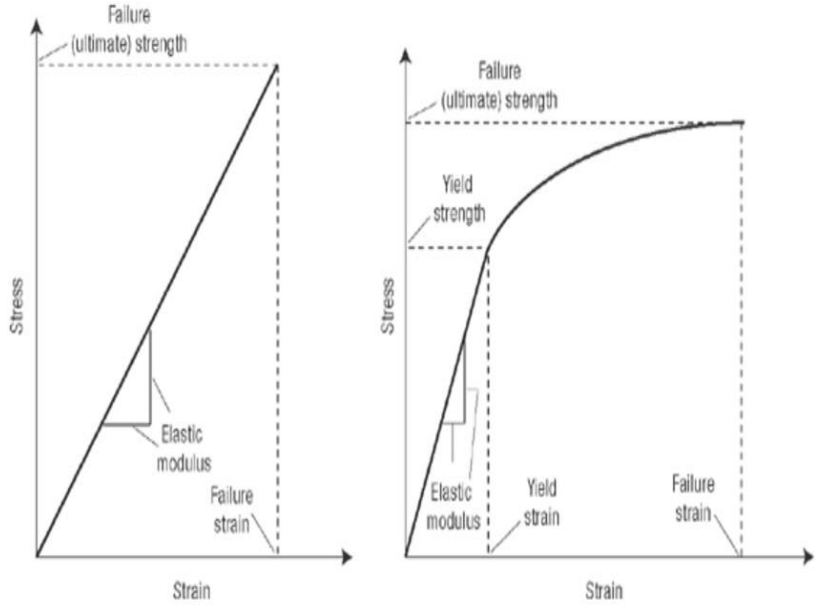

FIG. 14 SCHEMATIC STRESS-STRAIN CURVES FOR BRITTLE MATERIALS (LEFT) AND DUCTILE (RIGHT). FROM REFERENCE (27)

For the mainframe of the ground station, steel and aluminum were regarded in terms of strength, density, price and working conditions (since the ground station is meant to be used

outdoors). Both are ductile metals and depending on the alloy certain physical properties may be improved. The following is a brief overview of both metals and its characteristics:

Density

Steel's density, though may vary depending on the alloying elements (same as aluminum), usually has a density around 7.75-8.05 Kg/m^3. In general aluminum has a density of 2.70 Kg/m^3around (one third of steel's). This means that using the same volume of material, the weight of a steel structure would be substantially higher than the same structure made of aluminum.

Melting point

Melting point is dependent on the alloying elements but in both metals is way above the operating temperatures that can be reached even in the proximity of the servos, so no further study is made in this aspect.

Strength

As it happens with the melting point, the yield and tensile strength are heavily influenced by the alloying elements chosen. For example, the yield strength of aluminum may vary from 30 MPa to 500 MPa depending on the alloying elements and tensile strength may go from 79 MPa to 570 MPa. Same with steel, that can present a yield strength varying from 250 MPa to 1000 MPa and a tensile strength range between 400 MPa and 1250 MPa .

Regarding Young Modulus or elasticity modulus, which is a reference when evaluating the elastic behavior of the material, aluminum exhibits around 69 GPa where steel is usually around 210 GPa (28).

After reviewing the main characteristics of both steel and aluminum, it was decided to use steel for two main reasons:

Weight

A higher structural weight means the structure may not precise an anchorage or at least the dimensions of the counterweights would be smaller than the ones used with aluminum (even though an aluminum structure may present a better solution if the structure is going to be carried around in a vehicle).

Elasticity Modulus

A higher modulus means it's easier to operate in the elastic zone, preventing plastic deformations not desirable in any structure (plastic deformations may be microscopic, favoring appearance of microfractures inside the material and the apparition of cracks that can propagate and cause failure).

Since steel is susceptible to wear, a protective coating must be applied before putting the test bench to work. A zinc paint coating is enough to protect steel from corrosion, but if possible

a thermally conductive epoxy coating would be suggested since it will also protect the structure from abrasion and impacts. In Table 11 a summary with the mechanical properties to perform the structural analysis of the modules is offered. They will be used to define the material properties in CatiaV5, needed for presenting the maximum stresses and displacements.

TABLE 11 MECHANICAL PROPERTIES (STEEL)

Steel	
Density	7.86 Kg/dm^3
Yield Strength, S_y	250 MPa
Young Modulus, E	200 GPa
Ultimate Strength, S_u	420 MPa
Poisson Ratio, ν	0.266

3.7. Transmission Axis

After assuming the diameter of the axis, selecting the servomotor that will control the kite and having defined a material, the service life of the axis can be computed. For this, first a static analysis is carried out to check it won`t fail subjected to the stresses and, once provided it can withstand the moments induced by the tether and the servomotor, a fatigue analysis is also done to check how many service hours can last (and later compare them to the bearings and rails).

Before, the most demanding loading state of the axis must be evaluated. Since the tether is supposed to coil around the transmission axis, in the most demanding situation it will be subjected to a force perpendicular to its axis and displaced to the right or left a distance equivalent to its radius [6]. The transmission axis has a hole going through it, a keyhole to connect the servo and a diameter variation, conditions that must be taken into account when performing a fatigue study. In FIG. 15 the main dimensions of the axis can be observed.

[6] The diameter of the tether is disregarded

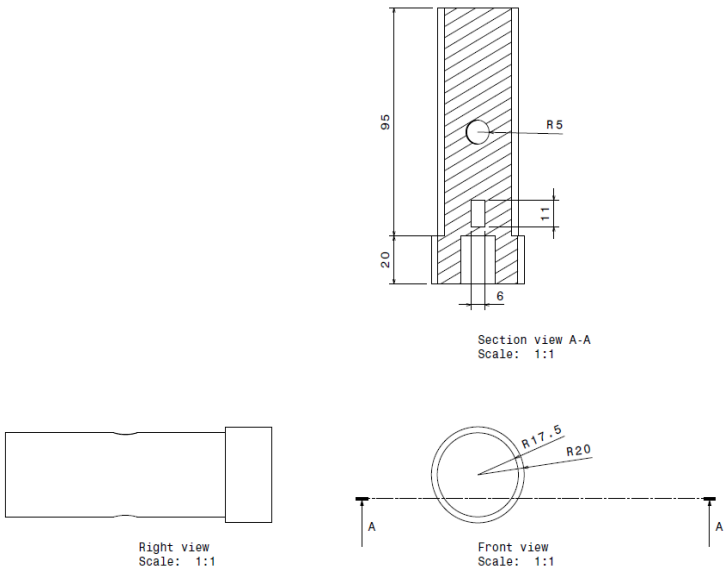

FIG. 15 TRANSMISSION AXIS – MAIN DIMENSIONS (CLIP FROM CATIAV5)

$$d_{ae} = 40\ mm;\ d_{ie} = 35\ mm$$

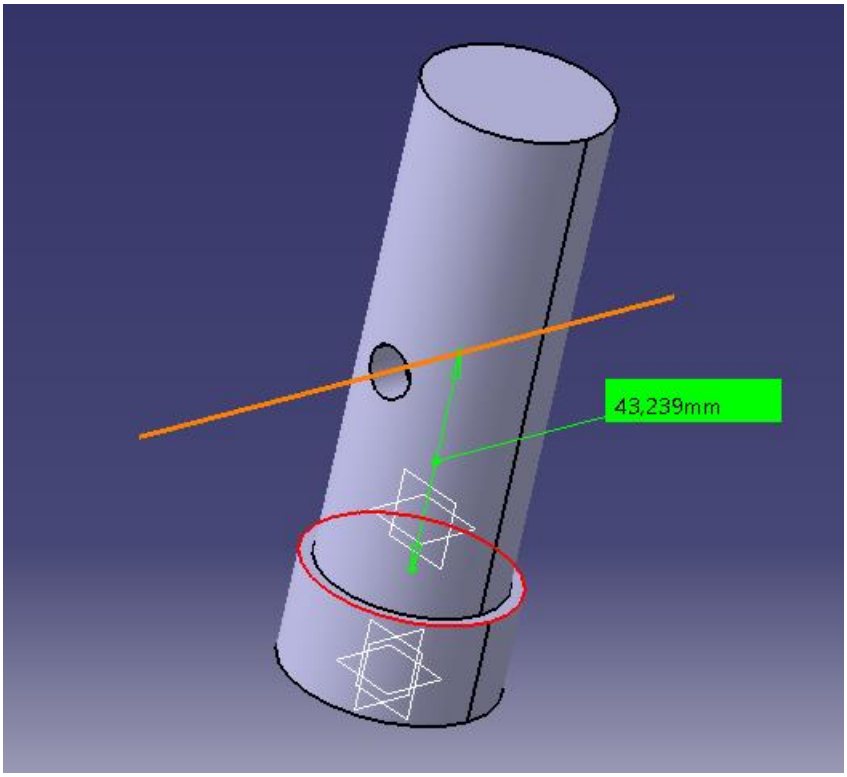

FIG. 16 TRANSMISSION AXIS

Static Study

Using the dimensions in FIG. 15 and 16, the values of the moments (bending and torque) can be defined since the tether force was previously calculated (page 19):

$$M_{ax} = F_{ss}\, t_a{}^{7} \quad (21)$$

$$T_{ax} = F_{ss}\, r_a \quad (22)$$

With M_a being the bending moment with a value of 45.69 Nm, and T_a being the torque, with a value of 17.67 Nm.

Once these values are known, to prevent static failure the following expression can be used (29):

$$2\sqrt{\left(\frac{16\mathrm{M_a}}{\pi \mathrm{d_a^2}} + \frac{2\mathrm{P_a}}{\pi \mathrm{d_a^2}}\right)^2 + \left(\frac{16\mathrm{T_a}}{\pi \mathrm{d_a^2}}\right)^2} \leq \frac{S_y}{n_s} \quad (23)$$

With $\mathrm{d_a}$ being the mean diameter of the transmission axis:

$$d_a = \frac{d_{ea} + d_{ia}}{2} \quad (24)$$

Where S_y can be found in Table 11, n_s from Table 3, d_{ea} and d_{ia} from FIG. 15 and $\mathrm{P_a}$ is the axis weight 6.27 N (obtained with CatiaV5). Since the diameter preliminarily chosen fulfills the requirements, the dynamic behavior can be checked.

Dynamic Study

For the dynamic check, it has been proven that the fatigue resistance of a transmission axis is not affected by the torque until $\tau_{max} = 1.5S_y$ (Sines Theory). The maximum shear stress can be computed as follows:

$$\tau_{max} = \frac{16T_{max}}{\pi d^3} \quad (25)$$

But, since the work aims to estimate the service life of the component, Goodman's Theory is going to be applied (using Von Mises criteria since it is more conservative than its alternative)

[7] Distance between the center of the hole and the part of the axis in contact with the upper plate surface.

$$d_a = \left[\frac{27.7 n_s}{\pi}\left(\left(\frac{T}{S_u}\right)^2 + \left(\frac{M}{S_f}\right)^2\right)^{1/2}\right]^{1/3} \quad (26)$$

With T and M defined as:

$$\frac{T}{S_y} \equiv \frac{T_a}{S_f} + \frac{T_m}{S_y} \quad (27)$$

$$\frac{M}{S_f} \equiv \frac{M_a}{S_f} + \frac{M_m}{S_y}^8 \quad (28)$$

And using (26), (26) and (26), S_f remains as:

$$S_f = 2.08\ MPa$$

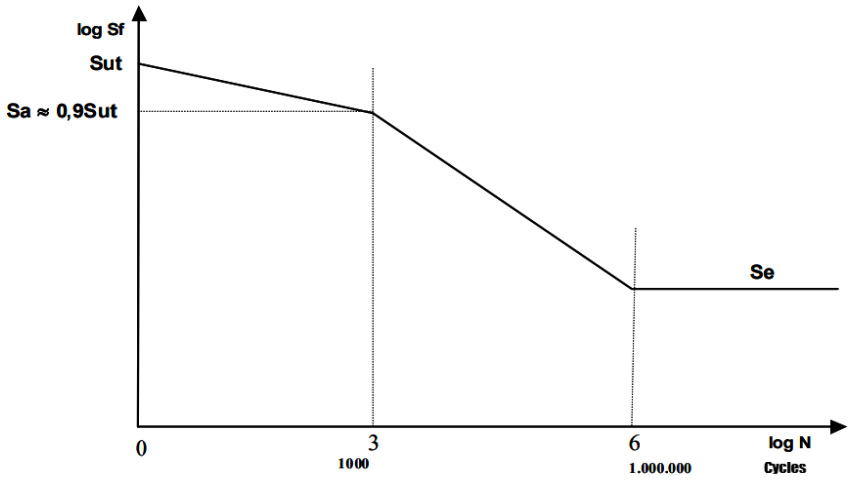

FIG. 17 S-N DIAGRAM

To know the number of cycles, first S_e must be known. It can be computed from Marin's equation:

[8] Both the subindex *a and m* make reference to the alternating and mean values of the bending moment and torque.

$$S_e = K_a K_b K_c K_d K_e K_f S'_e \quad (31)$$

After computing each of the coefficients, $S_e$would take the following value:

$$S_e = 231\ MPa^{9}$$

Once these values are known and with the S-N diagram, the service life of the axis would be:

$$\text{Service Life} = 1.212\text{E}6\ \text{cycles} = 400\ \text{h}^{10}$$

***

[9] For polished surface finish, 0.9 reliability.

[10] Assuming 3030 $cycles/hour$

4. FINAL DESIGN. CATIAV5 MODEL

CATIAV5 R21 is a powerful design software developed by Dassault Systèmes SE implemented since 1970 in the aeronautical industry at first and nowadays used in a wide variety of industries, from automotive industry (widely used in the Volkswagen Group among others) to construction, probably being the Guggenheim Museum in Bilbao one of the most famous projects in which CATIAV5 was used (30).

In this section, each component of the structure is presented and the corresponding structural analysis for the sheave holder, Module-I, Module-III and the union plate are performed since they are the components of the structure that should withstand the maximum loads and their failure mid operation may generate risks that can be avoided. The main condition for the analysis is that the yield strength of the materials is never exceeded so the structure stays operating in elastic regime, preventing plastic deformations.

4.1.Module-I

As it has been noted before in this document (see 1 ***Introduction***), this module is where the tether forces are redirected from the 3D space where the kite moves to the horizontal plane by means of sheaves, a moving sheave mounted on a holder and a static one that redirects the force directly to the load cell. Here is a review of each component:

4.1.1. Holder

This component maintains the sheave in its place, preventing the tether from moving freely and giving a better control of the kite's situation. FIG. 18 shows the design chosen for the holder as well as its expansion tree, showing the main operations performed to obtain the solid.

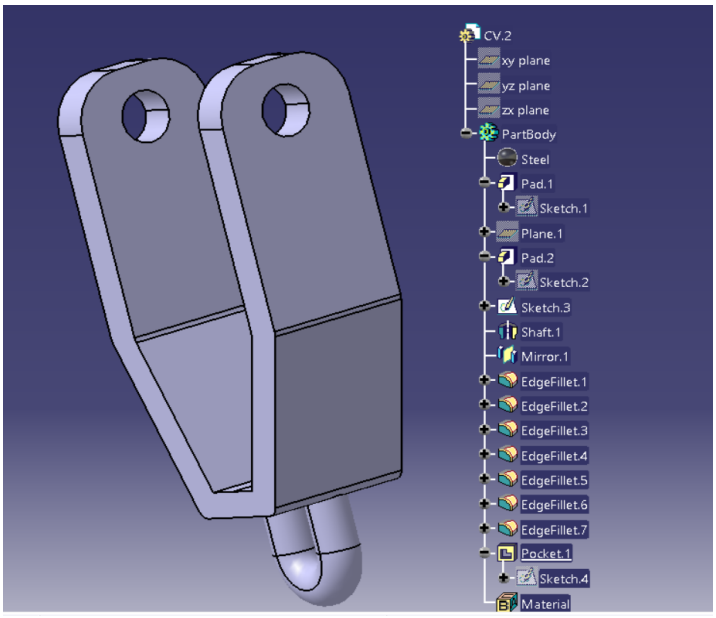

FIG. 18 HOLDER

4.1.2. Axis

For the moving sheave the axis has been designed using a simple geometry, with both ends having a wider zone to assure the sheave stays within the holder. In FIG. 19 the shape and operations for the creation of the axis can be observed.

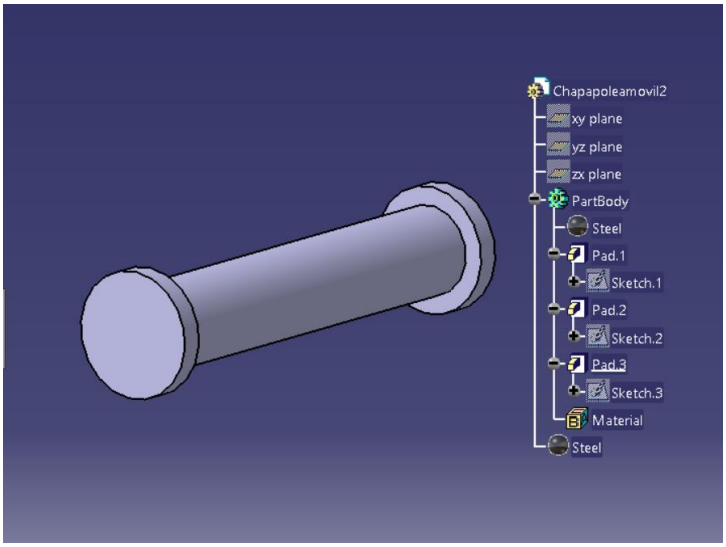

FIG. 19 SHEAVE AXLE

4.1.3. Sheave

The sheave is the only component of Module-I in which nylon instead of steel has been used. With this, less weight is put on the tether with the aim to restraint the minimum possible the movement of the kite. In FIG. 20 the main operations and the final shape of the sheave can be observed as well as nylon properties.

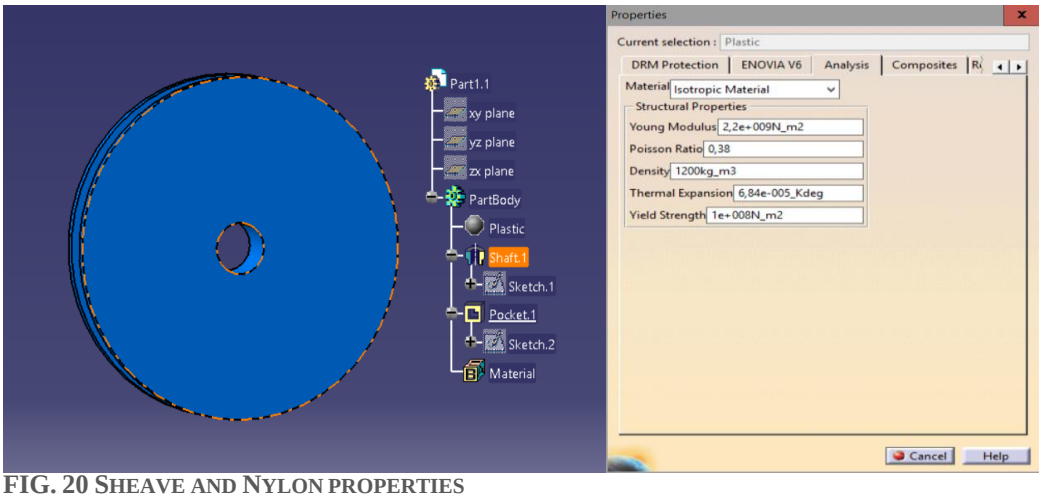

FIG. 20 SHEAVE AND NYLON PROPERTIES

4.1.4. Bushings

In this case, the bushing is a just a representation of the product previously chosen (See 3.3 *Bushings*, **Table 4**). FIG. 21 show the bushing and the mechanical properties of copper respectively.

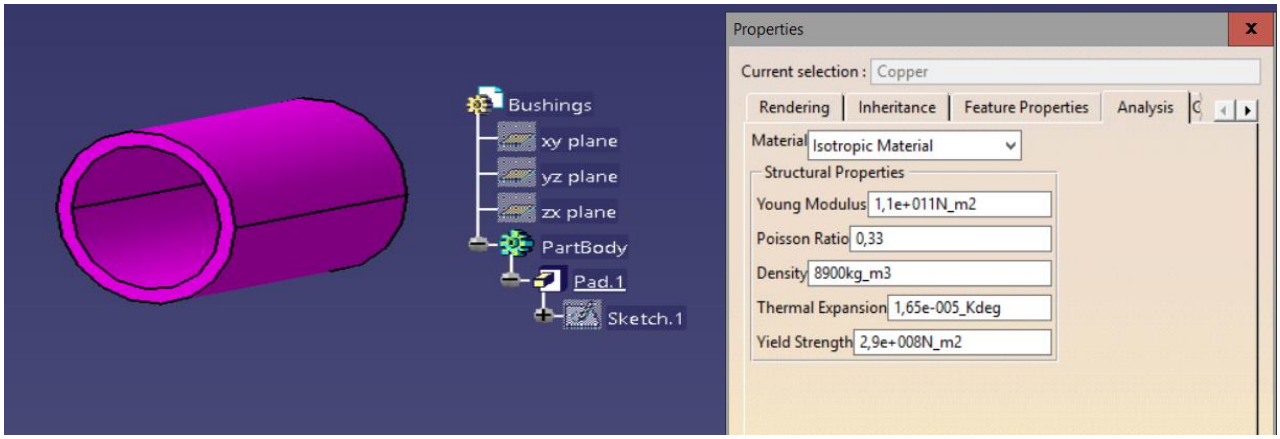

FIG. 21 BUSHING AND COPPER PROPERTIES

4.1.5. Top Plate

For the top part of Module-I, several factors have been taken into account:

- The horizontal sheave must be displaced with respect to the rail in Module-II a distance equal to the tread radius of the sheave, so the tether is aligned with the runner block and thus the force is transmitted with the less deviation possible.

- The height of the sheave has been taken into account with respect to the space the cell load would occupy.

- The holder should be as aligned with the horizontal sheave as possible for the same reason as the horizontal sheave must be relatively displaced from the rail.

- It must have an anchorage to fixate the holder.

- It must also have space for installing the horizontal sheave

With this conditions in mind the final geometry of the top plate remains as in FIG. 22 (SEE NEXT PAGE):

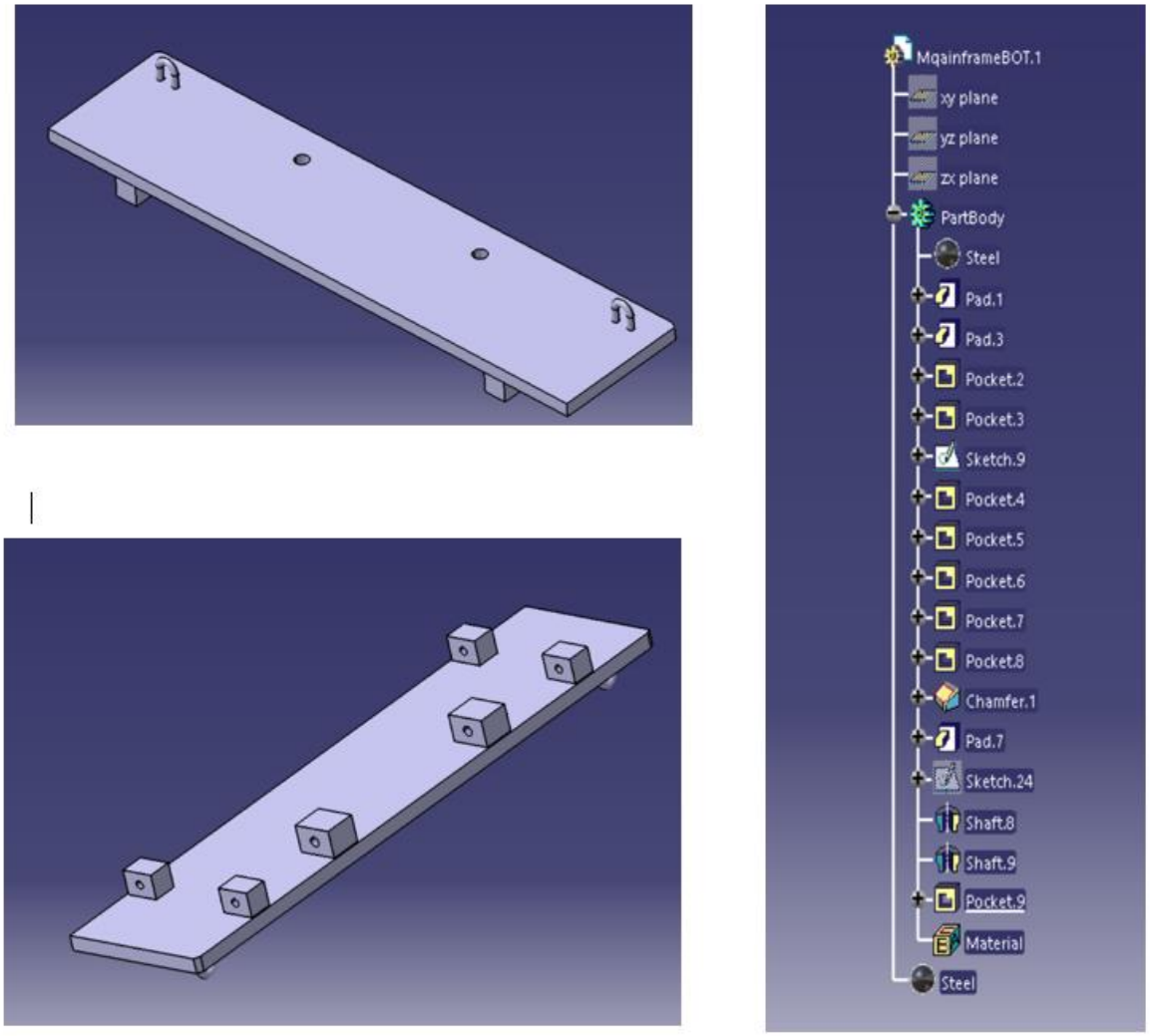

FIG. 22 MODULE-I TOP PLATE

4.1.6. Assembly Module-I

Once the main components of the Module are defined, the next step is to assemble all of them. Note that the bottom plate of Module-I has not been revised since it's a plain plate with just the protrusions for joining it to the top part (see 4.4.1 *Bars and Union Plate* to check the union bars and used for joining together both plates). In FIG. 23 a render from CATIA V5 of Module-I with all the elements assembled can be observed. As can be seen from the front

view of the render (left FIG. 23), there is enough space to place counterweights in case the kite could be expected to exert enough lift force to move the structure:

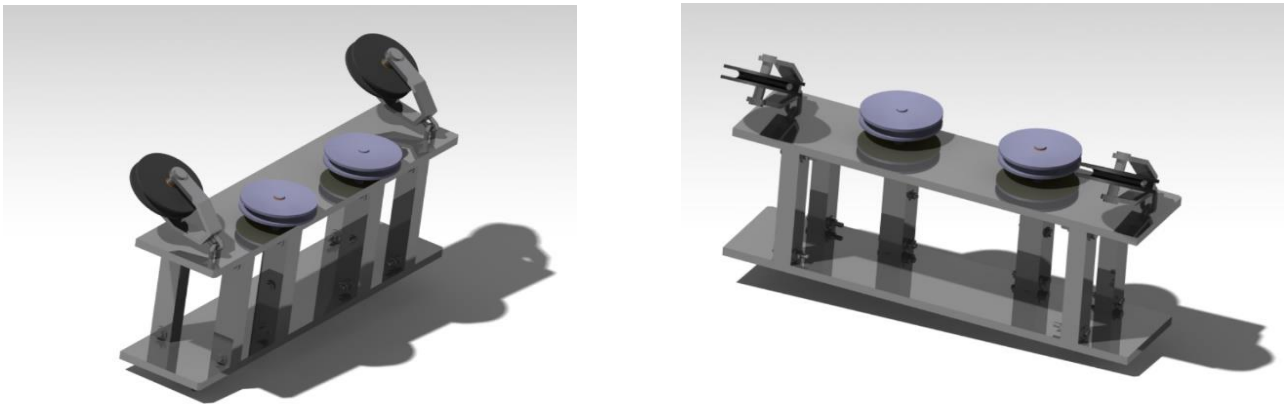

FIG. 23 MODULE-I RENDER

4.2. Module-II

This module is designed to hold the cell loads, withstand their weight and keep them restricted to a linear path (the total distance travelled is around 500 mm). It is the most lightweight part of the test bench, mainly because the bottom part has been devised in such a way that the minimum quantity of material has been used to prevent the structure from reaching a weight in which the reference car could not carry it whole.

4.2.1. Rails

As previously stated in 3.5.2 ***Rails***, these components must have a highly polished surface to ensure extended life service. In this application, since it will just be subjected to the cell load's weight, which is almost negligible in comparison to the loads the rail and runner block are designed to work with, service life is expected to be extremely long.
Since it will be operating outdoors, a strip cover for the bolts in order to prevent wear on the main parts of the rail is recommended[11].

[11] The cover strip is not represented in the CATIA model.

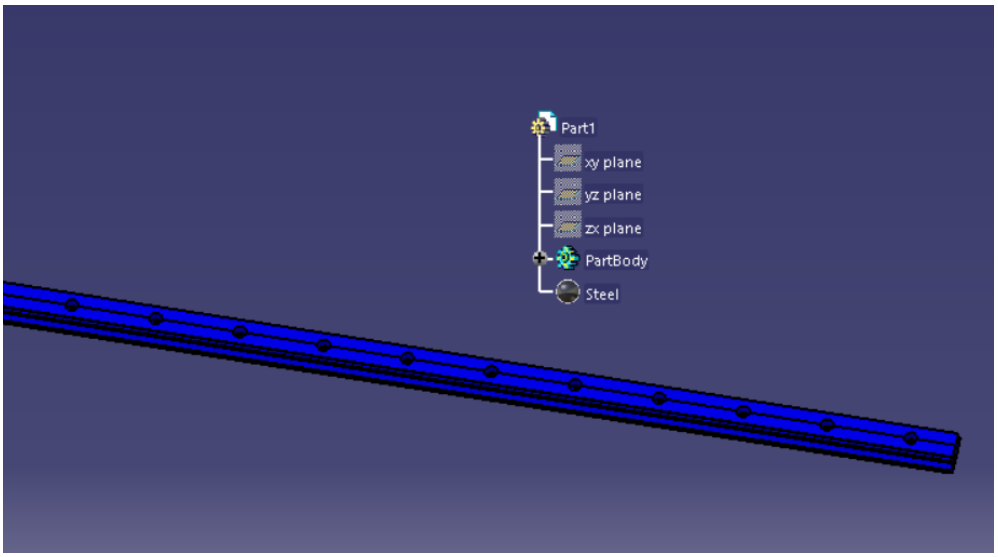

FIG. 24 RAILS FOR THE TEST BENCH

4.2.2. Runner Block

This component is the one that would be in charge of carrying directly the load. It has been designed in such a way that no matter the kind of cell load mounted, it should be relatively easy to secure it on top of the runner block. In this case use of auxiliary planes and symmetry operations have been used since the piece is a little bit more complex than the rest of the components reviewed so far (see FIG. 25). The complete assembly runner block / rail is depicted in FIG. 12

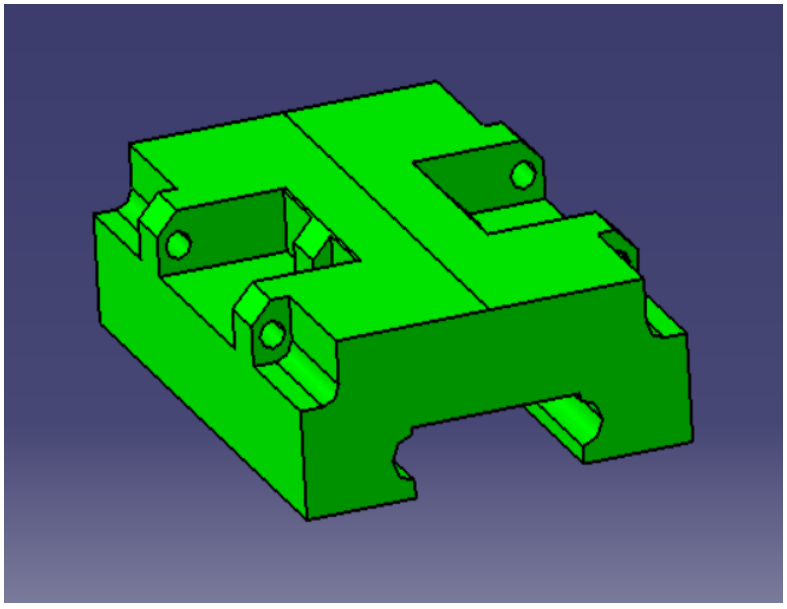

FIG. 25 RUNNER BLOCK

4.2.3. Assembly Module-II

Since the top plate and bottom plate of this module are relatively simple parts, the render of the full module is displayed in 31. As a remark, the top plate has drills along its length to allow a change of position of the rail or even a different kind of rail (provided the drills both in the new rail and plate are aligned allowing a clean and safe joining of both the structure and the product). Note the difference between the bottom part of this module and those of Module-I and III.

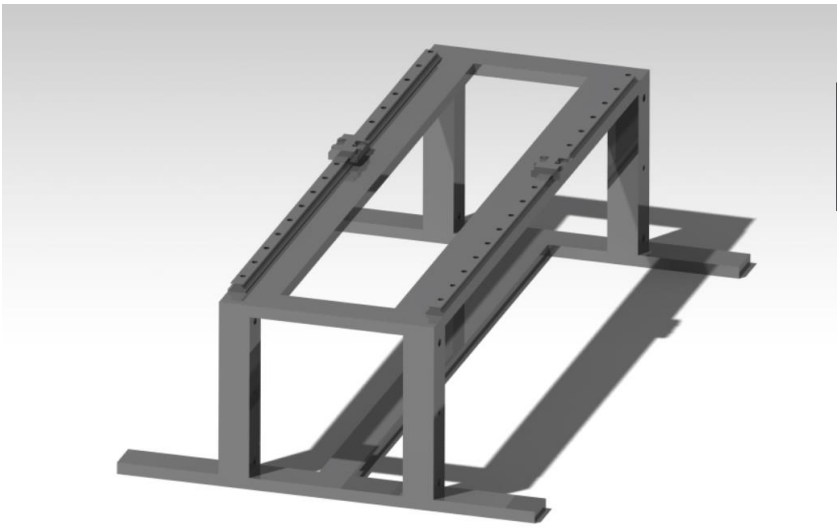

FIG. 26 MODULE-II

4.3.*Module-III*

This last module is the one with the most complexity and weight of the three. It has been designed in such a way the servomotors are joint to the top plate and most of their weight rests on silent blocks, to minimize the impact of the weight of the servomotors. It also has holes to mount the transmission axis and its bearings.

4.3.1. Transmission Axis

Its service life has been calculated in the previous chapter 4, were also a clip from the drawing shows the location of the keyhole to connect it to the servomotor. The wider part would be in contact with the inner ring of the bearing, avoiding unnecessary metal to metal contact. Also note that, as with the rails, the surface finish must be extremely fine. FIG. 27depicts the axis (another rendition of the axis has been seen in FIG. 10).

FIG. 27 TRANSMISSION AXIS

4.3.2. Servomotor

3D model provided by Omron. No modifications have been done to the CAD document provided by Omron (31).

FIG. 28 in next page shows a picture of the motor with the corresponding dependence tree.

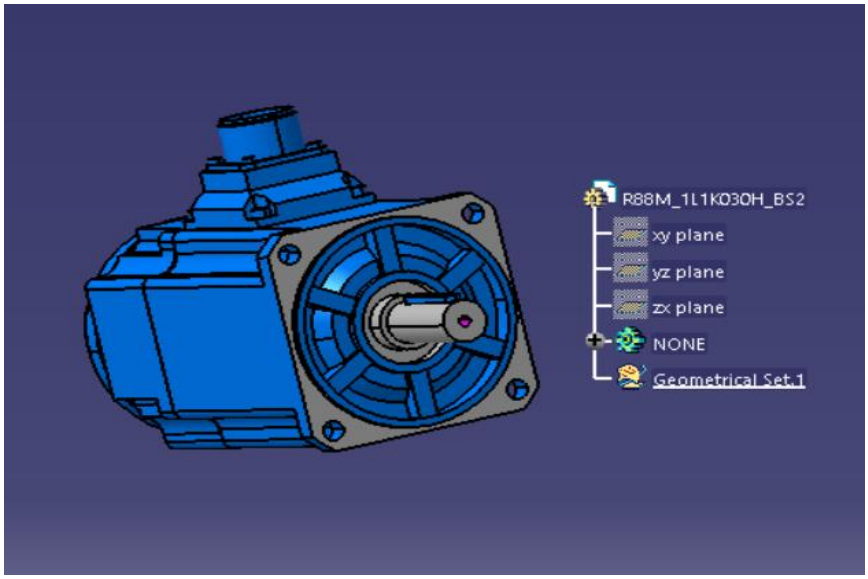

FIG. 28 SEVOMOTOR- OMRON

4.3.3. Bearings

As with the case of the servomotor, the CAD file has been obtained from the provider, SKF (32). Same as before, the geometry of the objects is not shown since it is external content.

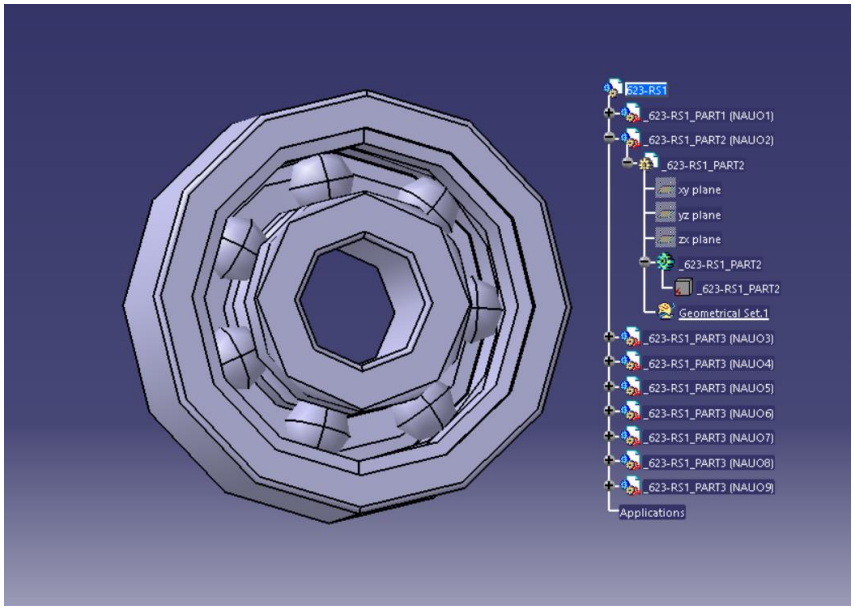

FIG. 29 BEARING-SKF

4.3.4. Silent Blocks

Silent blocks are machine components which usually help support a determined load and damper the vibrations, in this case, of the motor. They relieve stress from the top plate, since the weight of the servos wouldn't rest directly on the top plate but on the silent blocks. The selected product in for these servomotors would be from Silent flex, more accurately model 931147 (33).

4.3.5. Top Plate

This module includes orifices to install the bearings and transmission axis, as well as a geometry to secure the rear tethers. As can be seen in, a steel rod protrudes from the top surface. It is intended to use as a capstan, to reduce the forces to the axis and ensure the tether connects to the cell load in the appropriate dimension. Even though is not represented in the model, a plastic cover should be used as a capstan to reduce wear of the tether.

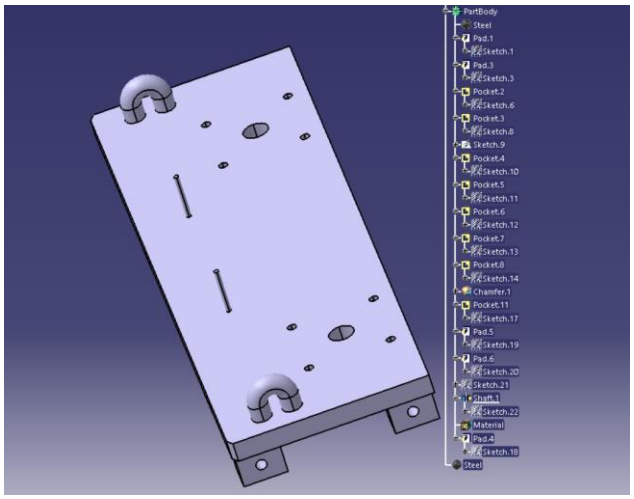

FIG. 30 TOP PLATE MODULE-III

4.3.6. Assembly Module-III

With all the components already mounted, Module-III would look like in FIG. 31 Module-III:

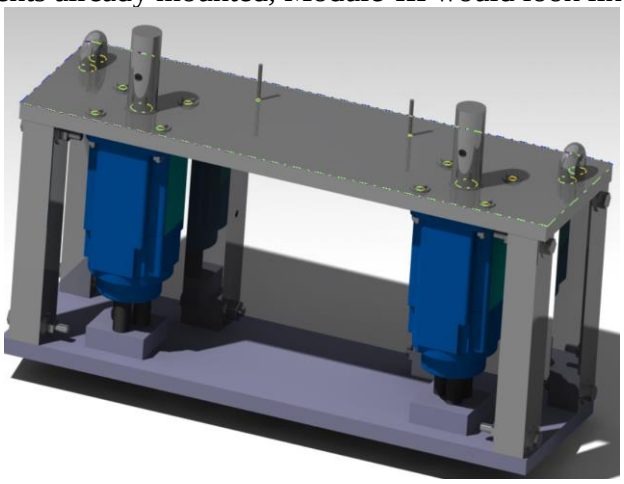

FIG. 31 MODULE-III

4.4. Connection Between Plates and Modules

In this section the connection bars between top and bottom plate, the union plates designed to act as union between modules and the bolts chosen for each connection are reviewed. Note that all the components are designed in steel, with a thickness of 2.5 mm and the bolts would be high resistance of class 10.9. In Table 12 the main mechanical properties of each bolt class are displayed.

TABLE 12 BOLTS PROPERTIES

Class	Prof Load $[MPa]$	Yield Strength $[MPa]$	Tensile Strength $[MPa]$
8.9	580	640	800
10.9	830	940	1040
12.9	970	1100	1220

4.4.1. Bars and Union Plate

Two different sections have been devised as can be observed in FIG. 32. Since the connections have been designed as bolted, M8 bolts for the 38x49, M12 for the 49x57 and M8 for the union plates (bolts have been chosen regarding the length of the screw shank according to ISO 4014).

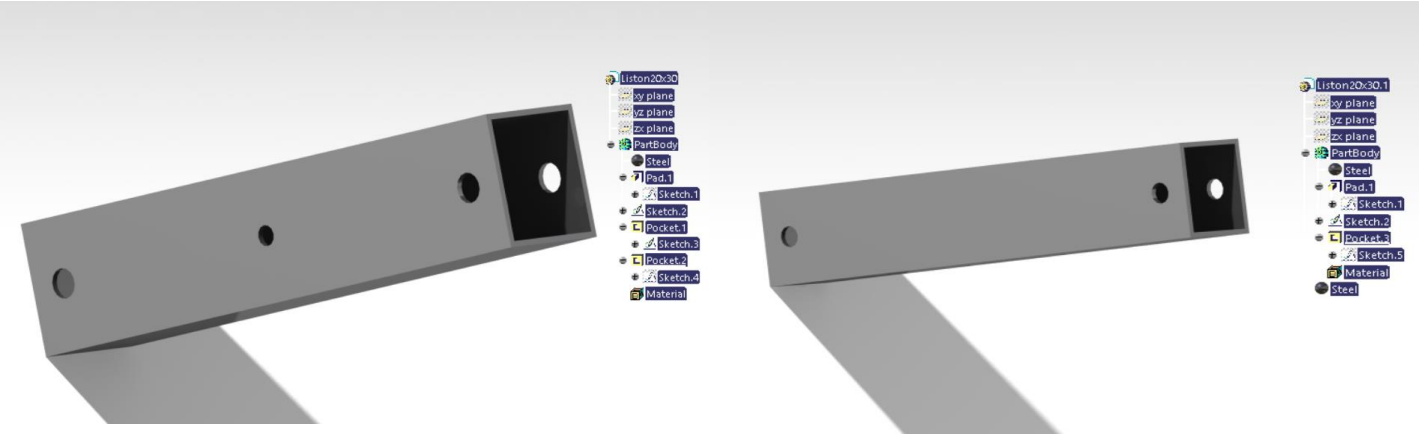

FIG. 32 SECTION 49X57 (LEFT) AND SECTION 38X49 (RIGHT)

4.4.2. Union Plate and Bolts

The union plates are pieces of steel shaped in such a way that two modules can be bolted together. They are joined by means of M8 bolts (as with the bars according to ISO 4014). The bolts used are shown in FIG. 34 with the following differentiation:

- A: Bolt M12
- B: Bolt M10
- C: Bolt M8
- D: Bolt M8 (servomotor)

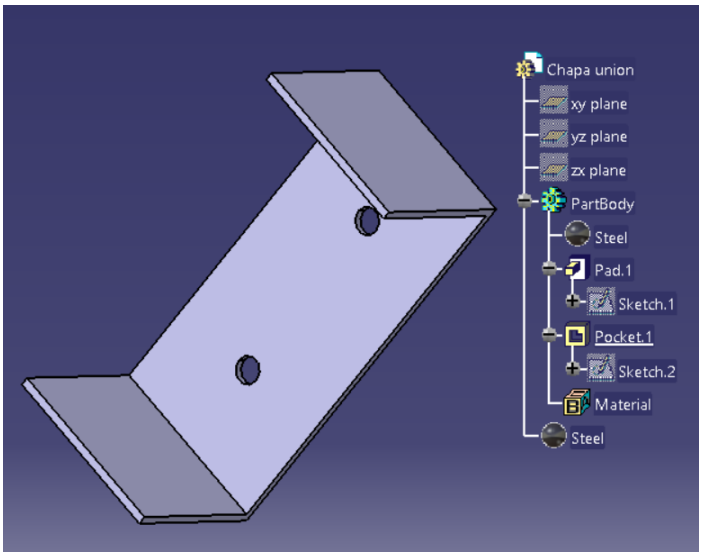

FIG. 33 UNION PLATE

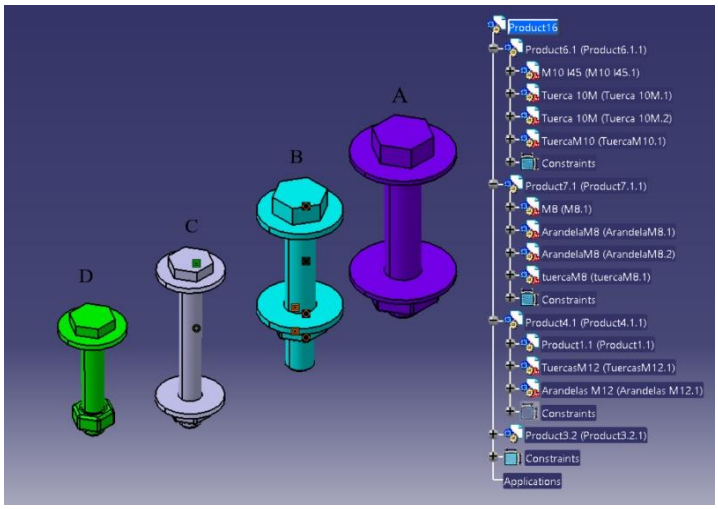

FIG. 34 BOLTS

4.5.Structural Analysis

After generating the components, a simplified structural analysis has been carried out for Module-I, Module-III, the sheaves and the union plate to check the behavior of the system and ensure no plastic deformation occurs according to Von Mises criteria, comparing the stress values obtained with the yield stresses of each material. Modifications from the preliminary design are done if the criteria are not fulfilled.

Also, three different models are studied for the sheave holder, selecting the one with the best behavior depending on the shape of the holder.

4.5.1. Module-I

This module, along with Module-III, is subjected to the main tether forces and reactions from the horizontal sheave axis. The simulation has been modeled pinning the base of the module and bolt bores that would joint together Module-I and II. With this, the stress values around the bolts connecting both modules, which are critical for the maintaining the integrity of the structure, can be known. For the analysis the structure has been modeled as one piece, taking into account the relative dimensions from the original piece such as bars thickness and holes for the bolts and sheave's axis dimensions.

Simulation Conditions

For the simulation, the force acting on the tether has been projected directly to the anchorage of the sheave holder and gravity taken into account ($10\ \frac{m}{s^2}$ as previously stated in Table 3) The input for the loads acting upon Module-I can be found in Table 3 (in page 21), and in 3.2.1 Sh*eave Load*, since the force exerted on the center of the sheave equals the reaction generated on the top plate of the structure where the sheave axis is connected to the structure. See FIG. 35

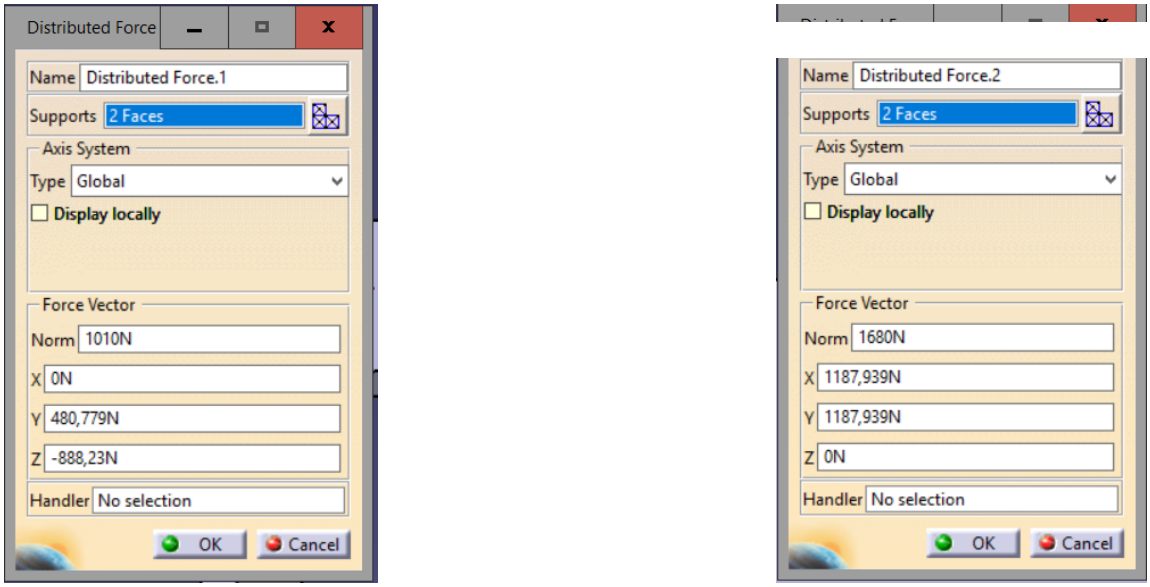

FIG. 35 FORCES FOR ANALYSIS

Clamping the point of the module that should be static, the structure before performing the analysis the forces, taking into account gravity, can be observed in FIG. 36

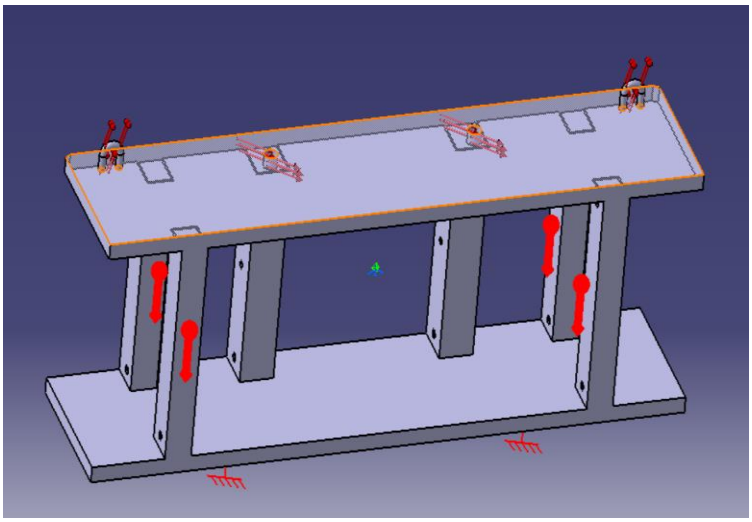

FIG. 36 ANALYSIS MODULE-I

From the report generated by CATIAV5 the total number of nodes, elements and mechanical properties of the module can be found in Appendix 1Appendi

The stresses and deformations have been simulated varying the bore were the 49x57 bars join the union plate. Since the 49x57 bars dimensions have been created regarding the normative for M12 bores, the variation of the initial M8 bore to a M10 does not make necessary any variations of the geometry. In FIG. 38 the maximum stresses generated in the structure are displayed for M10 (bottom) and M8 bores (top) respectively. In a close up of the bore from M10 can be observed in FIG. 37. As can be seen, the stresses have a variation of 1.2 MPa depending on the bore selected.

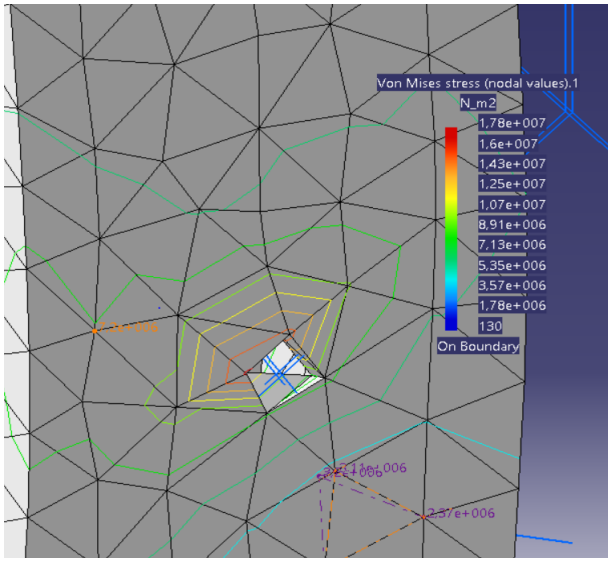

FIG. 37 M10 STRESSES

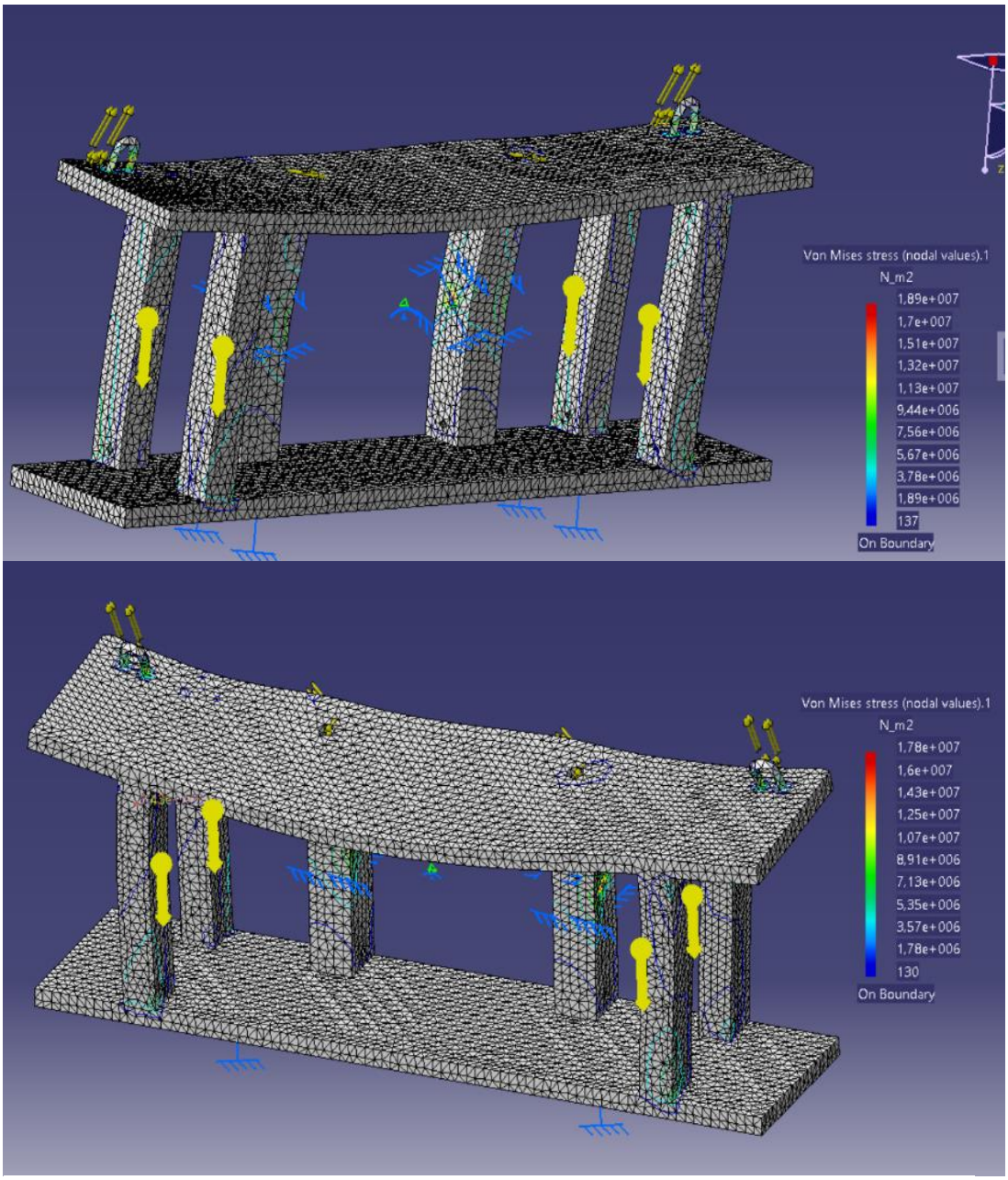

FIG. 38 STRUCTURAL ANALYSIS

The simulation of the plate has been carried out subjecting the piece to larger stresses (dimensioned to withstand the force of the tether on the contact surface) than it would have to withstand during operation as a safety measure to ensure no failure of this component during operation occurs, since it would present a serious safety problem (if the union were to fail and the kite exerted enough force to lift Module-I, it could be sent flying with the hazards derived from having an 80 Kg steel structure without control at a relatively high velocity). The predesign shown in FIG. 42 does not comply with the established condition and would surpass the yield strength around the corners of the M8 bore. For the final design, the thickness has been increased from 2.5 to 5 mm and the bore increased to the M10 bore.

In FIG. 39 the analysis for the definitive union plate can be observed and how the maximum strength does not surpass that of the yield strength in steel. The mesh analysis can be found in Appendix 3.

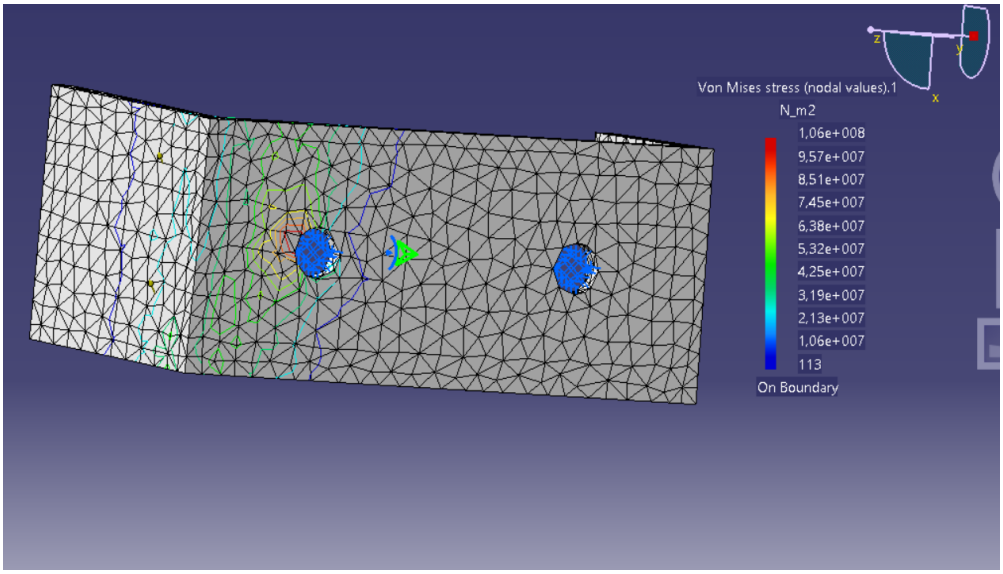

FIG. 39 UNION PLATE

4.5.2. Sheave and Sheave Holder

The sheave is the only component made of nylon. In FIG. 40 the stress analysis can be observed and how the maximum value obtained does not surpass that of the yield strength previously defined. In Appendix 4 information about the mesh and the analysis can be found.

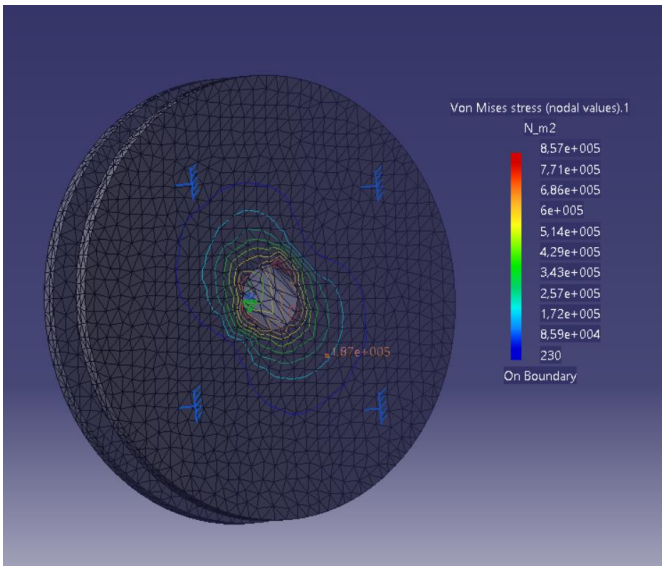

FIG. 40 MAX STRESS IN NYLON SHEAVE

For the sheave holder, a preliminary design was proposed and two alternatives with different geometries. In FIG. 41 the discarded designs can be appreciated.

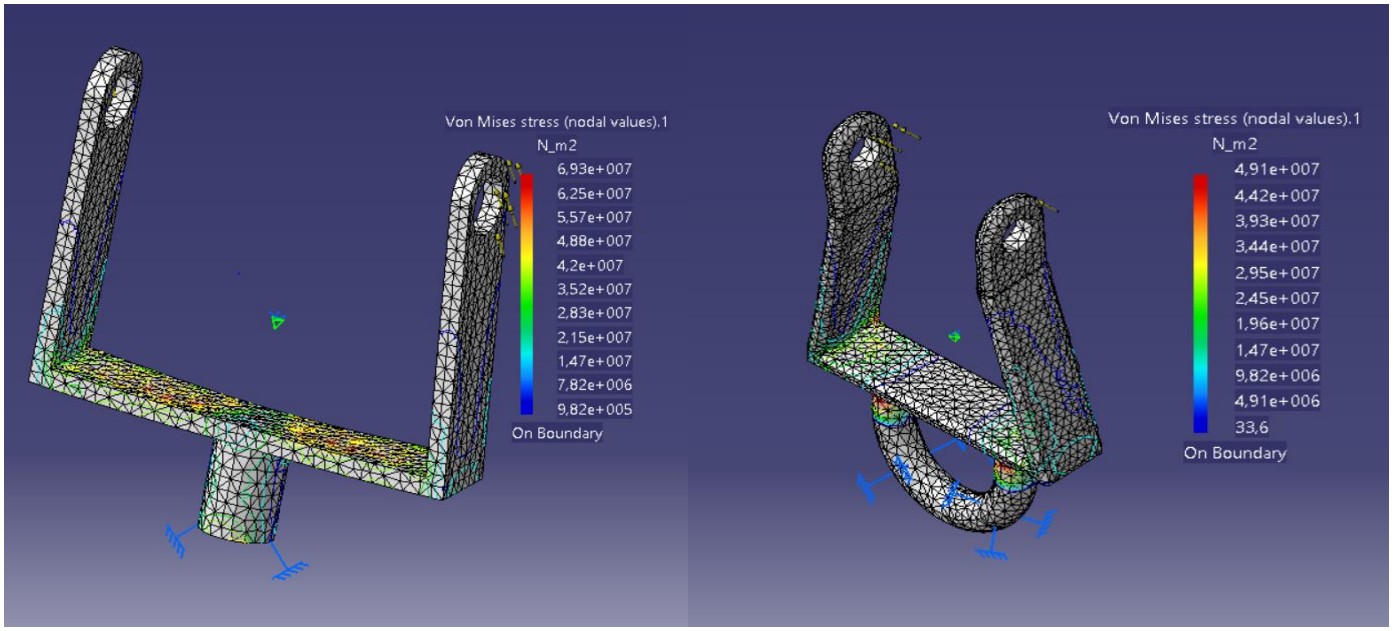

FIG. 41 HOLDER DESIGN ALTERNATIVES

From the three proposed models, and even though is not the one with the lower stresses, FIG. 42 has been chosen for geometrical reasons, since it is the model that best fitted with the top plate and maintains aligned the moving sheave with the horizontal sheave.

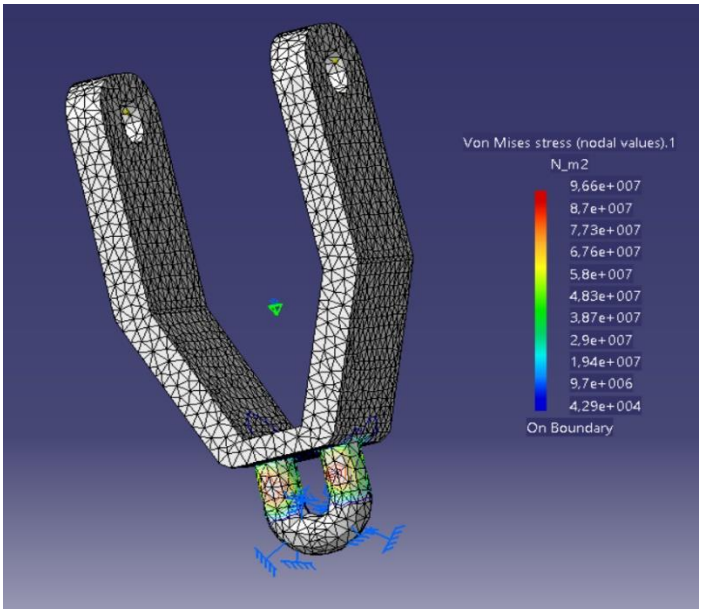

FIG. 42 FINAL DESIGN HOLDER

4.5.3. Module-III

For Module-III the load conditions are similar than those used for Module-I except from the stress applied where the transmission axis would be mounted. For simulating this, instead of a distributed load (which would be as in Module-I) the bearing reaction force is used. In Appendix 5 information regarding the mesh and properties can be found.

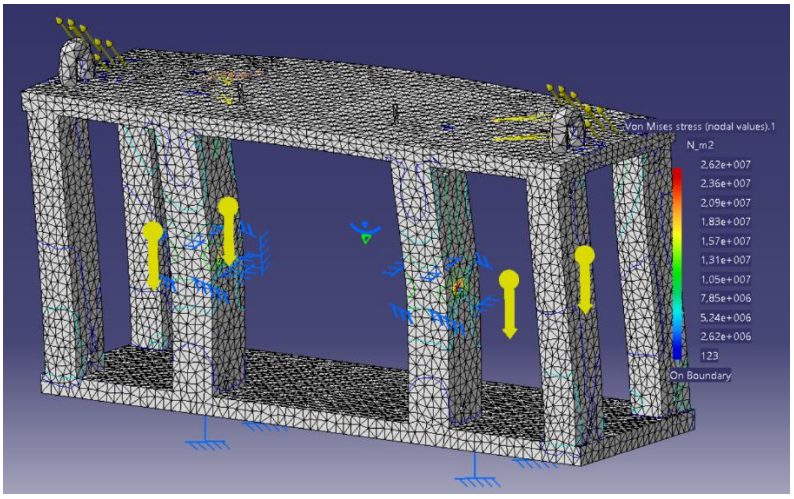

FIG. 43 MODULE-III STRESS ANALYSIS

5. BILL OF MATERIALS

In this chapter, a deeper analysis of the components in each module is presented. The total weight of each module and estimated prizing is also presented.

TABLE 13 MODULE-I COMPONENTS

MODULE-I

Components	Number	Lubrication	Materials	Surface Finish	Individual Weight	Total Weight
Bolts&Nuts	14	-	Steel	Fine		1,498
M12	4	-	Steel	Fine	0,137	0,548
M10	10	-	Steel	Fine	0,095	0,95
M8	-	-	Steel	Fine	-	-
Sheaves	4	-	Nylon	-	0,393	1,572
Holder	2	-	Steel	-	0,146	0,292
Long Axis	2	-	Steel	Extremely Fine	0,063	0,126
Short Axis	2	-	Steel	Extremely Fine	0,025	0,05
Top Plate	1	-	Steel	Fine	29,643	29,643
Bottom Plate	1	-	Steel	Fine	33	33
Union Plate	2	-	Steel	Fine	0,228	0,456
Bushings	4	Yes	Steel	Extremely Fine	0,04	0,16
Bars	6	-				4,36
49x57	2	-	Steel	Fine	1,09	2,18
38x48	4	-	Steel	Fine	0,888	3,552
					Total Weight	71.157

TABLE 14 MODULE-II COMPONENTS

MODULE-II

Components	Number	Lubrication	Materials	Surface Finish	Indiv Weight	Total Weight
Bolts&Nuts	18	-				2.046
M12	8	-	Steel	Fine	0,137	1,096
M10	10	-	Steel	Fine	0,095	0.95
M8	-	-	Steel	Fine	-	-
Rails	2	Yes	Steel	Extremely High	0,326	0,652
Runnerblock	2	Yes	Steel	Extremely High	0,01	0,02
Top Plate	1	-	Steel	Fine	33,63	33,63
Bottom Plate	1	-	Steel	Fine	23,016	23,016
Union Plate	4	-	Steel	Fine	0,228	0,912
Bars 49x57	4	-	Steel	Fine	1,09	8,72 4,36
					Total Weight	82.076

TABLE 15 MODULE-III COMPONENTS

MODULE-III

Components	Number	Lubrication	Materials	Surface Finish	Indiv Weight	Total Weight
Bolts&Nuts	22	-	Steel	Fine		1,538
M12	4	-	Steel	Fine	0,137	0,548
M10	10	-	Steel	Fine	0,095	0,95
M8	8	-	Steel	Fine	0,005	0,04
AC Drive	2	Yes			46,2	92,4
Top Plate	1	-	Steel	Fine	56,681	56,681
Bottom Plate	1	-	Steel	Fine	20,69	20,69
Union Plate	2	-	Steel	Fine	0,228	0,456
Bearings	2	Yes	Steel	Extremely Fine	0,04	0,08
Bars						4,36
49x57	2		Steel	Fine	1,09	2,18
38x48	4		Steel	Fine	0,888	3,552
					Total Weight	176,205

Regarding the total cost of the structure (estimate), and without taking into account manufacturing prices, knowing the servos cost (~ 8150 € each), bearings (~ 33 € each), bushings (~4 €), nylon and steel regarding current price market (e.g. linear meter of steel,

square section -steel EN 10209-, has a retail price in the line of 6 – 13 EUR plus VAT, depending on the supplier (for this estimate, as reference the prices appearing in (34) have been used) and on the total number of meters purchased. From (35), the average price of steel has been estimated as 3.26 €/kg.

Therefore, the total estimated cost of the materials (manufacturing / assembly costs not considered) is as follows:

Bearings(x2): 66 €

Bushings(x4): 16 €

Nylon (Sheaves x2): 40 €

OMRON Motor (x2): 16.300 €

Steel (plates & components): 661 €

Steel (supports): 160 €

TOTAL:17.243,00 €

***

6. CONCLUSIONS

As said in the preface ("Abstract"), this work aims to design a ground station helpful for the control of kites and for the measure of forces as accurately as possible to obtain, this within the area known as Airborne Wind Energy (AWE) SYSTEMS.

With the transition from fossil fuels to alternative energy sources, environmentally sustainable means for the production of electricity are growing at a very fast pace, especially wind and solar farms. In this aspect, AWE systems show a promising potential since winds at high altitudes, depending on the geographic location, show nearly constant behavior. Therefore, it is a matter of time (and money investment) that AWE systems enter in the list of real and efficient, alternate clean means of generating energy.

The design (modular, lightweight, easily transportable ground structure) is original and hence no comparisons with other designs have been included. The work presented herewith describes, in the author's opinion, the best possible solution ("rigid", one-piece structures, for example, have been also considered at the beginning of the works but discarded – not easy to transport and similar if not identical behavior e.g. when it comes to durability, and other factors).

No legal restrictive framework has been found with respect to the design of this particular device. Copyright and IP rights have been respected whenever required (e.g. the SKF catalog is protected by copyright, so references are made but no images copied). Whenever applicable, ISO and EN references have been used. All color Figures and tables shown have been created on purpose and specifically for this work by the author, by using CATIAV5.

As first stated in 2.1 *System Requirements***,** the current project has been devised trying to comply with all the conditions set in said chapter. All conditions have been met; however, there is still room for improvement and the system may be further optimized.

Having divided the structure in 3 modules, and since the whole structure mounted volume accounts for around 38 l, the only conditions that must be fulfilled to carry the test bench whole is that at least 1503.5 mm are available (since it is the length between the first edge of Module-I and the last of Module-III). For example, in the car taken as reference for

transportation, the test bench could be carried as a whole (the maximum width of the structure accounts for 860 mm). In any other case, one of the modules must be detached from the rest to fit.

Regarding service life and recommended components revision, the most conditioning element are the bearings, with a calculated 200 h, for which it would be advisable to perform evaluations of the components before reaching 200 h of service. Several bearings could be used for the system instead of the 61808, such as 61908, 16008 or 6008, which have a higher static and dynamic load capacity. If any of these bearings were to be used, the bore in the top plate of Module-III must be made wider and also the lubricant should be checked.

Also, as has been noted several times during the development of the work, all bearings and rails must be mounted with their respective seals, in the case of bearings, covers for the runner blocks and cover strips for the rails to prevent dirt and alien particles from damaging the highly polished surfaces needed for the correct operation of the test bench.

Regarding structural integrity, the preliminary design fulfills the requirements except for the union plate that had to be modified to cope with the stresses at which it was subjected. Even though those stresses were higher than the plate would be subjected to during operation, the analysis has been performed so the union between modules won't fail. For obtaining the desired outcome, the initial thickness of the plate has been increased to 5 mm, and the bolts, initially designed as M8, have been modified to M10 (with the dimensions modification associated with a bigger bore according to the regulation). In the case of the sheave holder, the geometry chosen is not the one that minimizes the stress but he one which best fits the design in terms of utility.

In all, the complete system constitutes a modular, transportable and solid test bench to control and measure forces in kite tethers, as a basis for an efficient and reliable ground structure to control an AWE kite.

***

7. BIBLIOGRAPHY

1. **World Bank Group.** ***World Bank Group.*** **[Online] 2016. https://datos.bancomundial.org/indicador/SP.POP.TOTL.**

2. World Health Organisation. WHO. [Online] 2016. http://www.who.int/mediacentre/factsheets/fs313/en/.

3. European Environmental Agency. ***Air Quality in Eruope.*** **2016.**

4. WHO and IEA . ***Forthcoming.*** **2016d.**

5. IEA. ***Tracking Clean energy Power 2017.*** **2017.**

6. ***Valuing the greenhouse gas emissions from nuclear power: A critical survey.*** **K.Sovacool, Benjamin. 2008, Elsevier, p. 14.**

7. ***Recent growth ad kock-on effects.*** **European Environment Agency. Cophenaguen : s.n., 2017. p. 74.**

8. ***Evaluation of global wind power.*** **Archer, Cristina L. and Jacobson, Mark Z. 2005, Journal of Geophysics.**

9. ***Crosswind Kite Power.*** **Loyd, Miles L. 1980, Journal of Energy, p. 111.**

10. ***Airborne Wind Energy Systems: A review of the technologies.*** **Cherubini, Antonello, et al. 2015, Elsevier.**

11. ***KiteGen: a revolution in wind energy generation.*** **Canale, Massimo, Fagiano, Lorenzo and Milanese, Mario. 2015, Elsevier, p. 1476.**

12. ***Developing a 600kW Airborne Wind Turbine.*** **Vander Lind, D. Delft, The Netherlands : s.n., 2015. Airborne Wind Enrgy Conference 2015.**

13. http://awec2017.com/. [Online] 2017.

14. ***Energy Policy.*** **Verbruggen, Aviel, et al. s.l. : Elsevier, 2009.**

15. ***Valuing the attributes of renewable energy investments.*** **Bergmann, Ariel, Hanley, Nick and Wright, Robert. Glasgow : Elsevier, 2004.**

16. ***Using conjoint analysis to quantify public preferences over the environmental impacts of wind farms. An example from Spain.*** **Álvarez-Farizo, Begoña and Hnaley, Nick. Glasgow : Elsevier, 2001.**

17. J. F. Manwell, J. G. McGowan, and A. L. Rogers. ***Wind energy explained: theory, design and application.*** **s.l. : Second Edi. John Wiley & Sons, 2009.**

18. ***Wind resource extrapolating tools for modern multi-MW wind turbines: Comparison of the Deaves and Harris model vs. the power law.*** **Gualtieri, Giovanni. 2017, Elsevier, p. 170.**

19. Datosclima.es. [Online] https://datosclima.es/Aemethistorico/Viento.php.

20. Ahrens, U.: Diehl, M.: Schmel, R. ***Airborne Wind Energy*** **. s.l. : Springer, 2013, p. 611.**

21. Timco, Inc. www.timco-eng.com. [Online]

22. SKF Group. ***SKF bushings, thrust washers and strips.*** **Sweden : s.n., 2010.**

23. https://industrial.omron.es/es/products. [Online] 2018.

24. SKF Group. Bearings. 2015. Vol. PUB BU/P1 10000/2 ES.

25. Bosch Rexroth AG. Ball rail systems. Scheinfurt, Germany : s.n., 2014. R999000485.

26. —. Miniature Ball Rail Systems. Schweinfurt, Germany : s.n., 2016. R999001207.

27. ***Nanomaterials: Nanotubes receak their true strength.*** **Stach, Eric. s.l. : Nature nanotechnology, 2008.**

28. ispatguru.com. [Online] 2018. [Cited: May 25, 2018.]

29. Tulio Piovan, Marcelo. Proyecto y calculo de Ejes y Elementos Accesorios. *Elementos de Máquinas.* 2004.

30. https://www.guggenheim-bilbao.eus/el-edificio/la-construccion/. [Online] 2018.

31. Omron. https://industrial.omron.es/es/services-support/technical-tools/cad-library. [Online] 2018.

32. SKF Group. http://www.skf.com/es/knowledge-centre/engineering-tools/skf-bearings-housings-units-and-seals-cad-models-general-instructions.html. [Online]

33. Silentflex. *Ariculaciones Elásticas.* Cantabria : s.n., 2018.

34. https://www.commentfer.es/. [Online] 6 5, 2018.

35. https://agmetalminer.com/metal-prices/stainless-steel/. [Online] 6 5, 2018.

36. Agency, International energy.

37. IEA. *Tracking Clean En.*

38. Rexroth. *Linear Motion Technology Handbook.* Germany : s.n., 2007.

39. *Influence of Hydrodynamic Journal Bearings With Multiple Slip Zones on Rotordynamic Behavior.* A.Bhattacharya, J.K. Dutt & R.K. Pandey. 2017, Journal of Tribology.

40. AST Bearings LLC. www.ASTBearings.com. [Online] 2012. https://www.astbearings.com/technical-information.html.

41. Ahrens, U.: Diehl, M.: Schmehl R. (Eds.).

42. *Social, economical and environmental impacts of renewable enrgy systems.* Akella, A. K., Saini, R. P. and Sharma, M. P. Jameshedpur, India : Elsevier, 2009.

43. http://www.premiumropes.com. [Online] [Cited: 4 25, 2018.] http://www.premiumropes.com/ropes-for-boats/kite-lines.

44. SKF Group. Skf Lubricants. 2018. PUB MP/P8 13238/2 EN.

****

8. APPENDIX

APPENDIX 1 MODULE-I MESH AND PROPERTIES

MESH:

Entity	Size
Nodes	18092
Elements	61690

ELEMENT TYPE:

Connectivity	Statistics
TE4	61690 (100,00%)

ELEMENT QUALITY:

Criterion	Good	Poor	Bad	Worst	Average
Stretch	61623 (99,89%)	67 (0,11%)	0 (0,00%)	0,269	0,563
Aspect Ratio	43384 (70,33%)	17337 (28,10%)	969 (1,57%)	6,142	2,307

Materials.1

Material	Steel
Young's modulus	2e+011N_m2
Poisson's ratio	0,266
Density	7860kg_m3
Coefficient of thermal expansion	1,17e-005_Kdeg
Yield strength	2,5e+008N_m2

APPENDIX 2 SHEAVE HOLDER MESH AND PROPERTIES

MESH:

Entity	Size
Nodes	2545
Elements	8778

ELEMENT TYPE:

Connectivity	Statistics
TE4	8778 (100,00%)

ELEMENT QUALITY:

Criterion	Good	Poor	Bad	Worst	Average
Stretch	8778 (100,00%)	0 (0,00%)	0 (0,00%)	0,317	0,659
Aspect Ratio	8533 (97,21%)	245 (2,79%)	0 (0,00%)	3,957	1,786

Materials.1

Material	Steel
Young's modulus	2e+011N_m2
Poisson's ratio	0,266
Density	7860kg_m3
Coefficient of thermal expansion	1,17e-005_Kdeg
Yield strength	2,5e+008N_m2

APPENDIX 3 UNION PLATE

MESH:

Entity	Size
Nodes	1911
Elements	6485

ELEMENT TYPE:

Connectivity	Statistics
TE4	6485 (100,00%)

ELEMENT QUALITY:

Criterion	Good	Poor	Bad	Worst	Average
Stretch	6485 (100,00%)	0 (0,00%)	0 (0,00%)	0,348	0,601
Aspect Ratio	5357 (82,61%)	1128 (17,39%)	0 (0,00%)	3,938	2,143

Materials.1

Material	Steel
Young's modulus	2e+011N_m2
Poisson's ratio	0,266
Density	7860kg_m3
Coefficient of thermal expansion	1,17e-005_Kdeg
Yield strength	2,5e+008N_m2

APPENDIX 4 SHEAVE MESH AND PROPERTIES

MESH:

Entity	Size
Nodes	5934
Elements	23281

ELEMENT TYPE:

Connectivity	Statistics
TE4	23281 (100,00%)

ELEMENT QUALITY:

Criterion	Good	Poor	Bad	Worst	Average
Stretch	23281 (100,00%)	0 (0,00%)	0 (0,00%)	0,380	0,651
Aspect Ratio	22714 (97,56%)	567 (2,44%)	0 (0,00%)	3,477	1,820

Materials.1

Material	Plastic
Young's modulus	2,2e+009N_m2
Poisson's ratio	0,38
Density	1200kg_m3
Coefficient of thermal expansion	6,84e-005_Kdeg
Yield strength	0N_m2

APPENDIX 5 MODULE-III MESH AND PROPERTIES

MESH:

Entity	Size
Nodes	17260
Elements	60486

ELEMENT TYPE:

Connectivity	Statistics
TE4	60486 (100,00%)

ELEMENT QUALITY:

Criterion	Good	Poor	Bad	Worst	Average
Stretch	60392 (99,84%)	94 (0,16%)	0 (0,00%)	0,265	0,561
Aspect Ratio	41590 (68,76%)	18142 (29,99%)	754 (1,25%)	6,649	2,371

Materials.1

Material	Steel
Young's modulus	2e+011N_m2
Poisson's ratio	0,266
Density	7860kg_m3
Coefficient of thermal expansion	1,17e-005_Kdeg
Yield strength	2,5e+008N_m2